

FINAL REPORT

Developing a Spatially Distributed Terrestrial Biogeochemical
Cycle Modeling System to Support the Management of Fort
Benning and its Surrounding Areas

SERDP Project RC-1462

DECEMBER 2010

Shuguang Liu
Larry L. Tieszen
USGS

Shuqing Zhao
Zhengpeng Li
ARTS

Jinxun Liu
SAIC and SGT

This document has been cleared for public release



This report was prepared under contract to the Department of Defense Strategic Environmental Research and Development Program (SERDP). The publication of this report does not indicate endorsement by the Department of Defense, nor should the contents be construed as reflecting the official policy or position of the Department of Defense. Reference herein to any specific commercial product, process, or service by trade name, trademark, manufacturer, or otherwise, does not necessarily constitute or imply its endorsement, recommendation, or favoring by the Department of Defense.

Table of Contents

Table of Contents	ii
List of Acronyms	iv
List of Figures and Tables	v
Acknowledgements.....	ix
Section 1 Executive Summary.....	1
Section 2 Objectives.....	3
Section 3 Background.....	4
3.1 Model System Development	4
3.2 Carbon Content in Forest Biomass	4
3.3 Simulating Soil Erosion and Deposition	5
3.4 Impacts of Cyclic Prescribed Fire on Ecosystem C and N Cycles	5
3.5 Differences in Carbon Sequestration Between Fort Benning and Surrounding Areas	6
Section 4 Materials and Methods	8
4.1 Study Area	8
4.2 Model System Development	8
4.2.1 GEMS	8
4.2.2 EDCM	14
4.2.3 Soil erosion and disturbance representations in GEMS.....	16
4.2.4 Data Preparation for Model Parameterization.....	17
4.2.5 Sensitivity Analysis	19
4.3 Fort Benning Forest States and Trends	21
4.4 Estimating Soil Erosion and Deposition	23
4.4.1 USPED	23
4.4.2 Determination of USPED Parameters at Fort Benning	25
4.4.3 Model Testing	27
4.5 Simulating Impacts of Cyclic Prescribed Fire on Ecosystem C and N Cycles.	27
4.5.1 The EDCM Model and Parameterization	27
4.5.2 Modeling Experimental Design and Analysis	28
4.6 Differences in Carbon Sequestration between Fort Benning and Surrounding Areas	30
4.6.1 LUCC Databases	30
4.6.2 Other Data Sources	30
4.6.3 Model Simulations	31
4.6.4 Analysis	32
Section 5 Results and accomplishments	33
5.1 Fort Benning Forest Status and Trends	33
5.2 Estimating Soil Erosion and Deposition	37
5.2.1 USPED Erosion Estimates and Comparison with Field Observations	37
5.2.2 Modeling Spatial and Temporal Changes of Soil Erosion and Deposition	39
5.3 Simulating Impacts of Cyclic Prescribed Fire on Ecosystem C and N Cycles.	40

5.3.1	Carbon and Nitrogen Fluxes	40
5.3.2	Carbon and Nitrogen Stocks	45
5.4	Differences in Carbon Sequestration between Fort Benning and Surrounding Areas	51
5.4.1	Comparisons of Spatiotemporal Patterns in Carbon Sequestration	51
5.4.2	Partitioning Carbon Sequestration	52
5.4.3	Differences between Fort Benning and Surrounding Areas	53
Section 6	Conclusions	55
References	57
Appendices	65
A.1	Supporting Data	65
A.2	List of Technical Publications	65
A.3	Other Technical Material	65

List of Acronyms

3PG	Physiological Processes Predicting Growth
ABGC	aboveground carbon
BA	basal area
BGC	belowground carbon
C	carbon
DBH	diameter at breast height (~1.3m above ground surface)
DI	disturbance index
EDCM	Erosion-Deposition-Carbon Model
EPA	Environmental Protection Agency
FORE-SCE	FOREcasting SCENarios of future land cover
GEMS	General Ensemble biogeochemical Modeling System
LAI	leaf area index
LUCC	land use and land cover change
MODIS	MODERate resolution Imaging Spectroradiometer
N	nitrogen
NPP	net primary production
NRCS	Natural Resources Conservation Service
RUSLE	Revised Universal Soil Loss Equation
SCS	Soil Conservation Service
SOC	soil organic carbon
SON	soil organic nitrogen
SSURGO	Soil Survey Geographic database
USDA	U.S. Department of Agriculture
USLE	Universal Soil Loss Equation
USPED	Unit-Stream-Power Erosion and Deposition
WEPP	Water Erosion Prediction Project

List of Figures and Tables

Figures:

Figure 1. Geographic location and topography of Fort Benning.	8
Figure 2. Diagram of the General Ensemble-based biogeochemical Model System (GEMS) and major steps in the spatial deployment of the encapsulated plot-level biogeochemical model over large areas.....	9
Figure 3. Interactions of the biogeochemical processes in the Fort Benning biogeochemical modeling system GEMS. Black arrows indicate mass flow and red arrows indicate control modifiers.....	10
Figure 4. Linking erosion/deposition model with biogeochemical model.	11
Figure 5. GIS coverages used in GEMS for building simulation units in the US Carbon Trends Project (Liu et al., 2004a). These GIS layers include land cover in the year 2000, climate polygons, soil map units, county boundary, and nitrogen deposition.	12
Figure 6. Diagram showing carbon cycling in a terrestrial ecosystem as simulated by the CENTURY and EDCM (Metherell et al. 1993). The algorithms shown here have been well tested worldwide. These established algorithms form the basis of a suite of terrestrial biogeochemical models, including CASA (Potter et al., 1993), InTEC (Chen et al., 2000), TRIPLEX (Peng et al., 2002), EDCM (Liu et al., 2003), and GEMS (Liu et al., 2004a).....	14
Figure 7. Diagram showing N cycling in a terrestrial ecosystem as simulated by the CENTURY and EDCM (Metherell et al. 1993). It can be seen that the N cycle is tightly coupled with the C cycle (Figure 6).....	15
Figure 8. Casual relationships of major disturbances with vegetation and soils in GEMS.	17
Figure 9. Estimated soil C of top layer (average 25 to 75 cm in thickness) at Fort Benning.....	18
Figure 10. Interpolated 1-km resolution monthly minimum temperature data for Fort Benning. The circles show the weather stations used for interpolation.	19
Figure 11. GEMS NPP sensitivity to model parameters.....	21
Figure 12. The spatial extents of the current and historical forest inventories.....	22
Figure 13. Relationship between stand basal area and total stand carbon density based on the current inventory.	22
Figure 14. Major C and N cycling processes and pools in the Erosion-Deposition-Carbon Model (EDCM).....	28
Figure 15. Comparison of GEMS NPP (Y) and MODIS NPP (X) in 2005 ($Y=0.99X$, $R^2=0.86$, $n=43166$).....	32
Figure 16. Distribution of tree density of Fort Benning forests around 2006. Tree density varied from 15 to 1,347 trees/ha across all the stands around 2006 with an average of 204 trees/ha.	34

Figure 17. Fort Benning forest age distribution according to the historical inventory. The youngest and oldest forests stands in the database were 1 and 332 years old, respectively, with an average age of 61 years old..... 34

Figure 18. Fort Benning forest biomass carbon distribution according to the historical inventory data. The minimum biomass carbon were 5.3 and 175.5 Mg/ha, respectively, with an average of 51 Mg/ha. 35

Figure 19. Comparison of forest age, basal area, and biomass carbon between the current and historical inventories. One dot represents one forest stand larger than 4 ha. 36

Figure 20. Age change (years) between the current and historical inventories. 36

Figure 21. Total biomass carbon change (Mg/ha) between two inventory databases... 37

Figure 22. Estimated overall soil rill erosions in ten watersheds. Each individual watershed had its own temporal change in erosion caused by differences in land cover change..... 38

Figure 23. Relationship of estimated rill erosion using USPED with observed stream water-suspended sediment. 38

Figure 24. Relationship of estimated rill erosion using USPED with disturbance index for ten watersheds at Fort Benning, GA. On the landscape or watershed scale, military disturbances were quantified using a disturbance index (DI) as defined by Maloney et al. (2005). 39

Figure 25. Spatial variation and temporal changes of soil erosion and deposition at two small watersheds at Fort Benning, GA. Display range is set to -1.0 to +1.0 ton/ha/yr to reveal spatial details of the majority of land pixels. Negative values indicate erosion. 39

Figure 26. Impacts of fire frequency, fire intensity, symbiotic and nonsymbiotic N inputs on net primary production (NPP) of ecosystem (a), tree canopy (b), and understory (c). Values within colored squares with different capital letters denote significant difference. 41

Figure 27. Long-term change trend in net primary production (NPP) of ecosystem (a), tree canopy (b), and understory (c) under four selected scenarios. The first number with scenario combination represents fire frequency, the second for fire intensity, the third f or symbiotic N input, and the fourth for nonsymbiotic N input. 1, 2 and 3 represents low, intermediate and high respectively. Insert numbers denote (r^2 , b)p, which follow the order of scenarios from top to bottom. The symbols for P value are the same as in Table 8. 42

Figure 28. Impacts of fire frequency, fire intensity, symbiotic and nonsymbiotic N inputs on total N input (a) and net N mineralization (b). Total N input includes symbiotic and nonsymbiotic N_2 fixation and atmospheric N deposition. Legends are the same as in Fig 26. 43

Figure 29. Long-term change trends in total N input (a) and net N mineralization (b) under the four selected scenarios. Legends are the same as in Figure 27. 44

Figure 30. Impacts of fire frequency, fire intensity, symbiotic and nonsymbiotic N inputs on forest ecosystem C stock (a), soil organic carbon (SOC) (b), understory aboveground C stock (c), and understory belowground C stock (d). Legends are the same as in Figure 26. 45

Figure 31. Long-term change trend in forest ecosystem C stock (a), soil organic carbon (SOC) (b), understory aboveground C stock (c), and understory belowground C stock (d) under the four selected scenarios. Legends are the same as in Figure 27.	48
Figure 32. Impacts of fire frequency, fire intensity, symbiotic and nonsymbiotic N inputs on forest ecosystem N stock (a), soil organic nitrogen (SON) (b), understory aboveground N stock (c), and understory belowground N stock (d). Legends are the same as in Figure 26.....	49
Figure 33. Long-term change trend in forest ecosystem N stock (a), soil organic nitrogen (SON) (b), understory aboveground N stock (c), and understory belowground N stock (d) under the four selected scenarios. Legends are the same as in Figure 27.	50
Figure 34. Spatial distributions of carbon (C) sequestration for Fort Benning (FB) and surrounding areas (SUR) during the periods 1992–2007 (current) and 2008–2050 (future). The inset graph denotes the area frequency distribution of C sequestration. A negative sequestration represents a movement of C from the landscape.	51
Figure 35. The contributions of net carbon (C) accrued in live biomass (b), forest floor (c), and soil (d) to ecosystem C sequestration (a).....	52
Figure 36. Temporal changes of annual precipitation (a) and mean annual temperature (b) for Fort Benning (FB) and surrounding areas (SUR) at present and in the future.	53
Figure 37. Current and future land cover dynamics for three major land cover types (forest, urban, and cropland) and transitional barren (caused primarily by forest harvesting) in Fort Benning and surrounding areas.	54

Tables:

Table 1. Forest age-class and biomass carbon lookup table (unit Mg C ha ⁻¹).....	13
Table 2. Values for some key inputs/parameters for the base run of the GEMS model.	20
Table 3. GEMS model sensitivity to key inputs/parameters. Values indicate relative change (%) to the reference run.....	20
Table 4. Table of Runoff Curve Numbers.....	26
Table 5. C-factor values for Fort Benning land cover types.....	26
Table 6. Experimental design for the combinations of fire frequency, fire intensity, and symbiotic and nonsymbiotic N inputs.	29
Table 7. Four scenarios for detailed analysis of C and N dynamics. The specifications of low, intermediate, and high are listed in Table 8.	29
Table 8. Basal area, biomass carbon, and number of trees by dominant species (total biomass C share >0.5 percent) at Fort Benning around 2006.....	33
Table 9. Comparison of basal area, age, and biomass carbon stocks derived from the current and historical forest inventories. (Note: the table largely reflects changes in the pine and mixed forests because the current inventory focused on these forests.)	35
Table 10. Standardized canonical coefficient of fire frequency, fire intensity, and symbiotic and nonsymbiotic N ₂ fixation rates for the prediction of NPP.	42

Table 11. Standardized canonical coefficients of fire frequency, fire intensity, and symbiotic and nonsymbiotic N ₂ fixation rates for the prediction of total N input and net N mineralization.	44
Table 12. Standardized canonical coefficients of fire frequency, fire intensity, and symbiotic and nonsymbiotic N ₂ fixation rates for the prediction of C stocks.	46
Table 13. Standardized canonical coefficient of fire frequency, fire intensity, and symbiotic and nonsymbiotic N ₂ fixation rates for the prediction of N stocks.	50

Acknowledgements

The Project (SI-1462) is supported by the Strategic Environmental Research and Development Program (SERDP), U.S. Department of Defense. We thank James Parker and other Fort Benning staff for providing the original forest inventory data. Valuable comments, suggestions, and logistic support from D. Imm, H. Balbach, J. Hall, and L. Mulkey are greatly appreciated. Work of S. Zhao was performed under USGS contract 08HQCN0007. Work of J. Liu was performed under USGS contract 03CRCN0001.

Any use of trade, product, or firm names is for descriptive purposes only and does not imply endorsement by the U.S. Government.

Section 1 Executive Summary

Military training activities can severely impact ecosystem structures, functions, health, and sustainability, which are intrinsically linked to ecosystem carbon (C) and nitrogen (N) cycles. Information on the impacts from military training activities on biogeochemical cycles is urgently needed for installation managers to minimize their adverse impacts on ecosystem services and sustainability.

Well-designed biogeochemical models can provide valuable quantitative information on the impacts of land use and climate variability on many ecosystem processes including the C and N cycles. Land and range managers at military installations need such information to strategically plan installation expansion and schedule training operations to prevent adverse environmental impacts from training.

This project, “Developing a Spatially Distributed Terrestrial Biogeochemical Cycle Modeling System to Support the Management of Fort Benning and its Surrounding Areas”, focuses on the development of a new biogeochemical modeling system. The overarching goal of this project is to develop an advanced, spatially distributed biogeochemical cycle modeling system to simulate the dynamics of ecosystem C and N cycles under historical, current, and future land use and disturbances scenarios. The modeling system and simulated results will be used to facilitate the evaluation of the environmental consequences of various training activities and, therefore, to support future land use and training operations.

Major findings from this project include the following:

Understanding the status and trends of forest resources and C fluxes and stocks is essential for forest management. We estimated C stocks for the inventoried forests using allometric equations, and found that the current inventory system can be improved for providing a complete dynamic picture of forest resource change in space and in time. We propose: (1) consider establishing a number of forest field plots that can be re-measured at an interval of less than 5 years. The forest stand change is best analyzed when such continuous measurements are available. (2) Key variables of forest stand should be monitored consistently, including tree height, DBH, density, canopy cover, dead wood, ground litter stock, major management/disturbance events, biomass removal, etc. (3) Any ground measurements (e.g. leaf area index, canopy cover, tree phenology) that helps to calibrate remote sensing observations should also be considered when applicable.

Military training activities may intensify soil erosion and deposition that contribute to the degradation of ecosystems. We used the Unit Stream Power-based Erosion Deposition (USPED) model to estimate the lateral movement of soils across Fort Benning. Land cover information derived from Landsat Thematic Mapper was used to estimate surface flow accumulation. Results from ten small catchments showed that simulated net erosion rates were significantly related to the observed total suspended sediments in stream water ($R^2 = 0.72$). Erosion estimates were also related to the land disturbance index that is a measure of the intensity of military training

disturbances. This suggested that the USPED model was an effective tool to quantify erosion and deposition at military installations.

Cyclic prescribed fire is essential to maintain and restore longleaf pine ecosystem and associated biodiversity. However, it also substantially alters ecosystem carbon and nutrient cycling processes. We simulated long-term ecosystem C and N dynamics at Fort Benning under impacts of different realistic combinations of fire frequency, fire intensity, symbiotic and nonsymbiotic N inputs, and N deposition using the Erosion-Deposition-Carbon Model (EDCM). Modeling results indicated that cyclic prescribed fire had significant impacts on long-term equilibrium status of C and N fluxes and stocks. Multiple regression analysis indicated that ecosystem NPP would be the lowest with high fire frequency and intensity without biological N inputs; without fire and with high levels of both symbiotic and nonsymbiotic N input, understory NPP would be the lowest. How fire affects the long-term ecosystem nutrient dynamics and how the ecosystem responds to fire depend strongly on both fire regime and N input from various sources. Practical scenarios with combined ecologically sound fire regime and appropriate management strategies were provided for maintaining and restoring longleaf pine ecosystem.

Military installations generally have substantially different land management strategies from surrounding areas, and the carbon consequences have rarely been quantified and assessed. We used the General Ensemble biogeochemical Modeling System (GEMS) to simulate and compare ecosystem carbon sequestration between the U.S. Army's Fort Benning and surrounding areas from 1992 to 2050. Our results indicate that the military installation sequestered more carbon than surrounding areas at present (76.7 vs. 18.5 g C m⁻² yr⁻¹ from 1992 to 2007) and in the future (75.7 vs. 25.6 g C m⁻² yr⁻¹ from 2008 to 2050), mostly because of differences in land use activities. Our results suggest that installations might play an important role in sequestering and conserving atmospheric carbon because some anthropogenic disturbances (e.g., urbanization, forest harvesting, and agriculture) can be minimal or absent on military training lands.

Based on those findings, we concluded that current management policies such as prescribed burning and vegetation conservation well maintain the Fort Benning ecosystem health and functions. Military training impacts on soil erosion is only at local scale compared to the overall conservation of the forest ecosystem. There is a need to update forest inventory monitoring with timely, high-resolution remotely sensed data in order to better capture the dynamic changes of forests.

The objectives of this project were met except for a fully spatially distributed computing mechanism. Key findings listed above were presented at meetings and published as peer-reviewed articles. The modeling system is packaged for Fort Benning end users. The model user can do model simulations using current database to evaluate consequences of carbon change under different climate and management scenarios.

The next step of this research will be focusing on (1) developing automatic linkage between USPED and GEMS, (2) a new interface for dealing with effective spatial simulations, such as using the NetCDF data, and (3) finalizing a complete GEMS documentation, including example data, manual and model code.

Section 2 Objectives

The overarching goal of this project is to develop an advanced, spatially distributed biogeochemical cycle modeling system to simulate the dynamics of ecosystem C and N cycles under historical, current, and future land use and disturbances scenarios. The modeling system and simulated results were used to facilitate the evaluation of the environmental consequences of various training and management activities and, therefore, to support future land use and training operations. This report describes the major accomplishments of this project. Our major research objectives were to:

- Develop an advanced, spatially distributed biogeochemical cycle modeling system for Fort Benning ecosystems and its surrounding areas.
- Depict Fort Benning forest conditions from the forest inventory data that were collected during 1981–2000, and in 2006. Compare forest stands common in the two datasets to infer recent forest changes. Relations of forest biomass to forest basal area are used to derive forest biomass change between the two inventories.
- Find ways to represent military land surface disturbances in the simulation of soil erosion and deposition, and evaluate the suitability of USPED at Fort Benning by simulating the spatial distribution of erosion and deposition within ten watersheds using total suspended sediments measured in the runoff.
- Use the EDCM to simulate the long-term ecosystem C and N dynamics at Fort Benning under the impacts of different combinations of fire frequency, fire intensity, symbiotic and nonsymbiotic nitrogen inputs, and nitrogen deposition. Specifically, we sought to 1) examine the effects of cyclic prescribed burning on plant production, soil nutrient cycling, and net N mineralization rates; 2) present the consequences of ecosystem C and N dynamics following current fire regime; and 3) provide a scientific basis and practical scenarios for land management decisions in determining ecological sound fire regimes, and appropriate management strategies for maintaining the ecosystem sustainability at Fort Benning.
- Use GEMS, which is capable of dynamically assimilating LUCC information into the simulation process over large areas, coupled with a yearly LUCC database and corresponding climate and soil data to simulate and compare spatiotemporal patterns in ecosystem carbon sequestration between the Fort Benning installation and surrounding areas from 1992 to 2050.

Section 3 Background

Well-designed biogeochemical models can provide valuable quantitative information on the impacts of land use and climate variability on many ecosystem processes including the C and N cycles. Land and range managers at military installations need such information to strategically plan installation expansion and schedule training operations to prevent adverse environmental impacts from training.

Our research activities mainly concentrated in five areas: (1) develop an advanced, spatially explicitly biogeochemical cycle modeling system for Fort Benning, (2) spatially and explicitly estimate carbon stocks in tree biomass and their change over time, (3) improve USPED model simulations of soil erosion and deposition by incorporating remotely sensed data, (4) simulate the impacts of cyclic prescribed burning on ecosystem C and N fluxes and stocks, and (5) simulate and compare spatiotemporal patterns in ecosystem carbon sequestration between the Fort Benning installation and surrounding areas from 1992 to 2050. The background of these research activities are described below.

3.1 Model System Development

Many biogeochemical models are capable of simulating ecosystem C-N cycles. However, most of them are not capable of simulating the impacts of soil erosion and deposition because most biogeochemical models do not consider C-N movements on landscape. On the other hand, many empirical- and process-based soil erosion and deposition models have been developed, but most of them do not have detailed simulation of C-N cycles of vegetation and soil. For the Fort Benning area, this is the first attempt to build a spatially explicit modeling system that combines the strengths of both model types.

Here we first describe our GEMS modeling framework and its embedded biogeochemical model EDCM. In this study, EDCM and GEMS were used as the prototype models for applications at the plot and regional scales, respectively. Then we reviewed existing soil erosion-deposition models that would be suitable for incorporation into GEMS and EDCM.

3.2 Carbon Content in Forest Biomass

The status and dynamics of forest conditions at Fort Benning, related to changes of many ecosystem goods and services, are a major concern for installation managers and the general public. Although the forests have been periodically inventoried in the past, no systematic effort has been made to estimate forest biomass or carbon content in forest biomass and its change in space and time. Such information is essential to assess the efficacy of current forest inventory system, understand the status and trends of forest change, evaluate the effectiveness of forest resource management practices and severity of training impacts, and serve the various purposes of scientific research activities (e.g., parameterize ecosystem models and constrain model projections).

3.3 Simulating Soil Erosion and Deposition

Military training installations typically host activities such as ground infantry training and maneuvers of tracked and wheeled vehicles. Some of these activities can have severe impacts on the structure of vegetation and soils, leading to accelerated soil erosion on the landscape. Severe soil erosion reduces on-installation ecosystem productivity and the rate of subsequent ecosystem recovery. In addition, severe erosion and deposition is a major concern for off-installation neighboring regions and down-streams. Fort Benning, Georgia, is a highly active military training post. Much of the training conducted at Fort Benning involves tracked vehicles. The soils at Fort Benning are characterized by a very fine sand/clay texture, which is susceptible to erosion especially after mechanical disturbance (Hahn et al., 2001). Research activities have been deployed to determine disturbance threshold, monitor water quality, and quantify erosion at Fort Benning (SEMP annual report, 2003).

In order to formulate management decisions to follow regulations on preventing excessive soil erosion and deposition, and maintain ecosystem health to support the long-term sustainability of military training functionalities at the installation, it is necessary to quantify and predict the dynamics of soil erosion and deposition on the landscape of military installations. Accurate predictive quantification helps to identify potential erosion and deposition sites and allows land managers to focus resources on problem areas (Zaluski et al., 2003).

A suite of models has been developed to simulate soil erosion and deposition, ranging from empirical (e.g., USLE and MUSLE at <http://www.iwr.msu.edu/rusle/>) to largely physically-based models (e.g., WEPP at <http://topsoil.nserl.purdue.edu/nserlweb/weppmain/wepp.html>). USLE or MUSLE are capable of estimating soil erosion and have been widely tested on agricultural landscapes. WEPP is a physically-based process model that simulates both erosion and deposition. Its application might be hampered by its complexity and requirements on many spatial data layers. USPED is a simpler model than WEPP, but is capable of simulating the spatial distribution of erosion and deposition with the assumption of a steady overland flow under uniform rainfall excess conditions (Mitasova et al., 1996; Mitas and Mitasova, 1998). Although the assumption is seldom satisfied, recent applications of USPED at several locations demonstrate that USPED can simulate erosion and deposition reasonably well (Blanco and Nadaoka, 2006; Warren et al., 2005; Pistocchi et al., 2002; Alimohammadi et al., 2006; Zaluski et al., 2003). Nevertheless, its feasibility for application at military training settings has not been evaluated.

3.4 Impacts of Cyclic Prescribed Fire on Ecosystem C and N Cycles

Periodic fire was historically an integral component of the pine ecosystems in the Southeastern United States (Christensen, 1987; Gilliam and Platt, 1999), and prescribed fire has been widely implemented for fuel reduction (Wagle and Eakle, 1979), competition control (Brockway and Lewis, 1997; Glitzenstein et al., 2003), and wildlife habitat management (Noss, 1989; Kwilosz and Knutson, 1999; Madden et al., 1999). However, frequent fire may result in ecosystem nitrogen (N) deficiency due to repeated N loss through combustion, volatilization, and leaching (Neary et al., 1999; Reich et al., 2001), thereby presenting a challenge for maintaining ecosystem

sustainability. On the other hand, fire may stimulate the abundance and diversity of herbaceous legumes and resultant symbiotic N₂ fixation activity (Waldrop et al., 1992; Towne and Knapp, 1996; Hendricks and Boring, 1999; Hiers et al., 2000, 2003; Newland and DeLuca, 2000). In addition, some studies have documented that nonsymbiotic N₂ fixation is a key process for maintaining the storage of N in regularly burned ecosystems (Eisele et al., 1989; DiStefano and Gholz, 1989; Bormann et al., 1993). Given these opposite consequences of prescribed burning, the issue of how prescribed fire influences N balance and ecosystem sustainability has received increasing attention. Unfortunately, surprisingly few studies have examined the integrated effects of cyclic prescribed fire, biological N₂ fixation and atmospheric N deposition on the long-term dynamics of nutrient cycling and plant production in regularly burned pine forest ecosystems.

Prescribed fire, a common forest management practice throughout the Southeast, has been used at Fort Benning for two purposes. First, prescribed fire is required to maintain and restore fire-adapted pine communities that are a critical habitat for the federally endangered red-cockaded woodpecker (*Picoides borealis*) and gopher tortoise (*Gopherus polyphemus*). Second, it removes the ground layer plants to facilitate military training access. However, the long-term impacts of fire management on C and N cycles and ecosystem sustainability have not been quantified. Recently, Garten (2006) used a simple compartment model to predict the effects of prescribed burning at Fort Benning without considering biological nitrogen input, such as symbiotic and nonsymbiotic N₂ fixation; this could lead to significant biases both in scientific research and land management decisions since biological N₂ fixation may play an important role in replenishing N loss from fire.

3.5 Differences in Carbon Sequestration Between Fort Benning and Surrounding Areas

Land use and land cover change (LUCC), which directly affects the biogeochemical interactions between the terrestrial biosphere and the atmosphere (Schimel et al., 2001; Houghton and Goodale, 2004), is responsible for large carbon fluxes in and out of terrestrial ecosystems (Fang et al., 2001; Houghton, 2003; Kauppi et al., 2006). To accurately quantify the geographic distributions, magnitudes, and mechanisms of terrestrial carbon sequestration at local to global scales, it is critical to estimate the carbon exchange between the terrestrial biosphere and the atmosphere because of LUCC. However, it has been a primary challenge to quantify the carbon exchange between the land and atmosphere induced by LUCC in regional and global carbon cycle studies (Houghton et al., 1999; Prentice, 2001; Achard et al., 2004; Ramankutty et al., 2007), mainly due to the lack of detailed LUCC databases and appropriate models capable of dynamically assimilating land use change information into the simulation process over large areas. Consistent, high-quality, and spatially explicit LUCC databases, combined with appropriate modeling techniques, may provide the best approach for accurately quantifying regional terrestrial carbon sequestration patterns.

Military installations offer a special case for examining how LUCC can affect biological carbon sequestration because these lands generally have substantially different land management strategies from surrounding areas and the military can adopt proactive management approaches (Baskaran et al., 2006). Unfortunately, there have been few studies conducted to quantify and

assess the carbon consequences in military installations, especially the biological carbon sequestration potential in the future.

Here, we used GEMS, which is capable of dynamically assimilating LUCC information into the simulation process over large areas, coupled with a yearly LUCC database and corresponding climate and soil data to simulate and compare spatiotemporal patterns in ecosystem carbon sequestration between the Fort Benning installation and surrounding areas from 1992 to 2050. Four counties, Muscogee, Marion, Chattahoochee and Russell, were selected to compare with Fort Benning. This is because these counties surround the Fort Benning installation and have very different land cover management from that of the Fort Benning.

Section 4 Materials and Methods

4.1 Study Area

Fort Benning is located in the Southwest of Georgia, U.S.A., covering an area of about 730 square kilometers (Figure 1). It has a sub-tropical climate with a mean annual temperature of 18.3 °C and annual precipitation of 1300 mm. Soil textures are mainly sand and sandy loam at ridges and hillslopes and sandy loam and sandy clay in the valleys. The very fine-grained sand/clay soils are highly erodible (Hahn et al. 2001). Land cover at Fort Benning consists of 49% mixed forests, 25% deciduous, 7% evergreen, and 10% barren (Garten and Ashwood, 2004a). Training activities are diverse, but involve primarily the maneuver of tracked vehicles. Prescribed burning and forest thinning are commonly employed for ecosystem management (SEMP annual report, 2003).

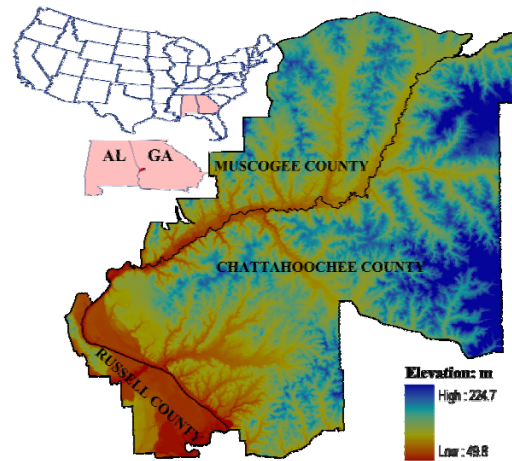


Figure 1. Geographic location and topography of Fort Benning.

4.2 Model System Development

4.2.1 GEMS

4.2.1.1 General Framework

Many plot-scale process-based biogeochemical models have been developed during the past 20 years (Parton et al., 1987; VEMAP Members, 1995; Schimel et al., 2000; Chen et al., 2000; McGuire et al., 2001). However, few of the models have the capability of dynamically assimilating land cover and land use information into the simulation processes over large areas (Schimel et al., 1991; Potter et al., 1993; Melillo and others, 1995; McGuire et al., 1997; Pan et al., 1998; Chen et al., 2000).

GEMS (Liu et al., 2004a, Liu et al., 2004b) is one of the few models that can be used to predict the impacts of natural processes, management practices, and land uses on biogeochemical cycles

over large areas. It has been used to investigate the carbon and nitrogen dynamics in various ecoregions of the United States, such as the Southeastern Plains, the Appalachians, and the Northwest Great Plains. The impacts of many driving forces, including land cover and land use change (LUCC), climate change and variability, atmospheric N deposition, CO₂ fertilization, chemical fertilization, and fire on carbon and nitrogen dynamics are being investigated using GEMS (Liu et al., 2004a).

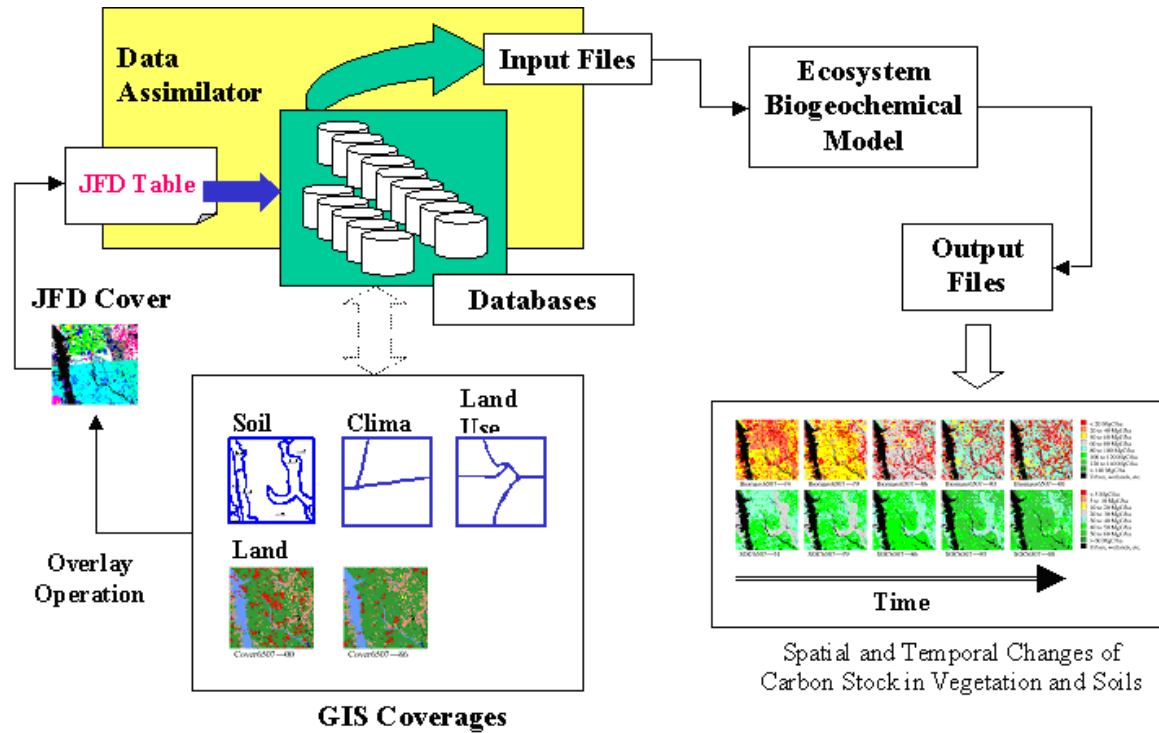


Figure 2. Diagram of the General Ensemble-based biogeochemical Model System (GEMS) and major steps in the spatial deployment of the encapsulated plot-level biogeochemical model over large areas.

GEMS is a modeling system that was developed for a better integration of well-established ecosystem biogeochemical models with various spatial databases (Figure 2) (Liu et al., 2004a, 2004b). It consists of three major components: one or multiple encapsulated ecosystem biogeochemical models, a data assimilation system (DAS), and an input/output processor (IOP). The DAS can search and retrieve information from various databases according to the keys provided by a joint frequency distribution (JFD) table of the major environmental driving variables (Reiners et al., 2002; Liu et al., 2004a). JFD is a product obtained using a map overlay operation, in which land pixels are clustered into unique simulation units bearing the same environmental conditions, such as soil property, vegetation, climate, and disturbances. The smallest JFD could be the size of a single pixel on the most fine resolution input map (e.g., 30m resolution land cover grid) whereas the largest JFD could be the size of a single pixel on the coarsest resolution input map (e.g., 10km climate grid). The implementation of the JFD concept in GEMS reduces the computation burden.

For each JFD, GEMS downscales the regional scale information to the field scale using a Monte Carlo ensemble approach, which incorporates the variability (as measured by variances and covariance) of the driving variables of the underlying biogeochemical models into simulations, and thus is capable of providing uncertainty estimates of the predicted variables in time and space. Monte Carlo methods are applied at the beginning of simulations, but it has effects at each of the time steps, such as the pre-determined crop rotation of each year. The field scale data are then injected into the modeling processes through the IOP which updates the default input files. Values of selected output variables are also written by the IOP to a set of output files.

The interactions of generic biogeochemical processes in GEMS are shown in Figure 3. The C cycle is the main flow of GEMS. The C cycle starts from GPP and NPP calculations, then C allocation, litterfall, mortality, and finally to soil C decomposition. The C cycle is tightly coupled with and influenced by the N cycle and the water cycle as indicated by the red arrows in Figure 3. The water cycle includes algorithms to estimate rain interception, evaporation, transpiration, runoff, and soil water content. The water cycle is linked with soil organic C decomposition and plant growth through soil water availability. The N cycle is coupled with the C cycle through N availability, which controls both plant growth and soil carbon decomposition. External driving forces are climate, and human and natural disturbances.

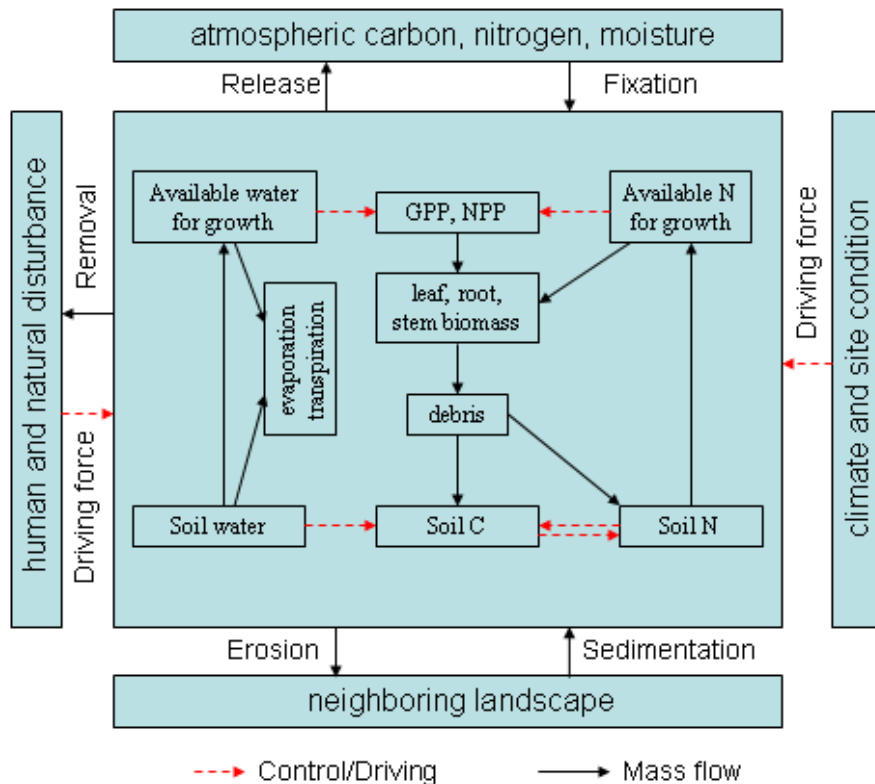


Figure 3. Interactions of the biogeochemical processes in the Fort Benning biogeochemical modeling system GEMS. Black arrows indicate mass flow and red arrows indicate control modifiers.

Military training activities typically cause vegetation destruction, soil physical changes, and enhanced erosion and deposition in training areas. Soil erosion and deposition affect soil profile evolution, spatial distribution of carbon and nutrients, and ecosystem dynamics. We use the USPED model (Mitas, and Mitasova, 1998) to quantify erosion and deposition. The approach of linking soil erosion and deposition with GEMS biogeochemical simulation is shown in Figure 4.

The spatial resolutions of the digital elevation model (DEM), together with climate, soil, vegetation, and management maps, dictated the spatial resolution for USPED deployment. The erosion and deposition rates simulated by USPED were grouped into discrete classes. The map showing these classes are included in the generation of the JFD for Fort Benning. Losses of C and N during lateral sediment transportation will be accounted for using an oxidation factor.

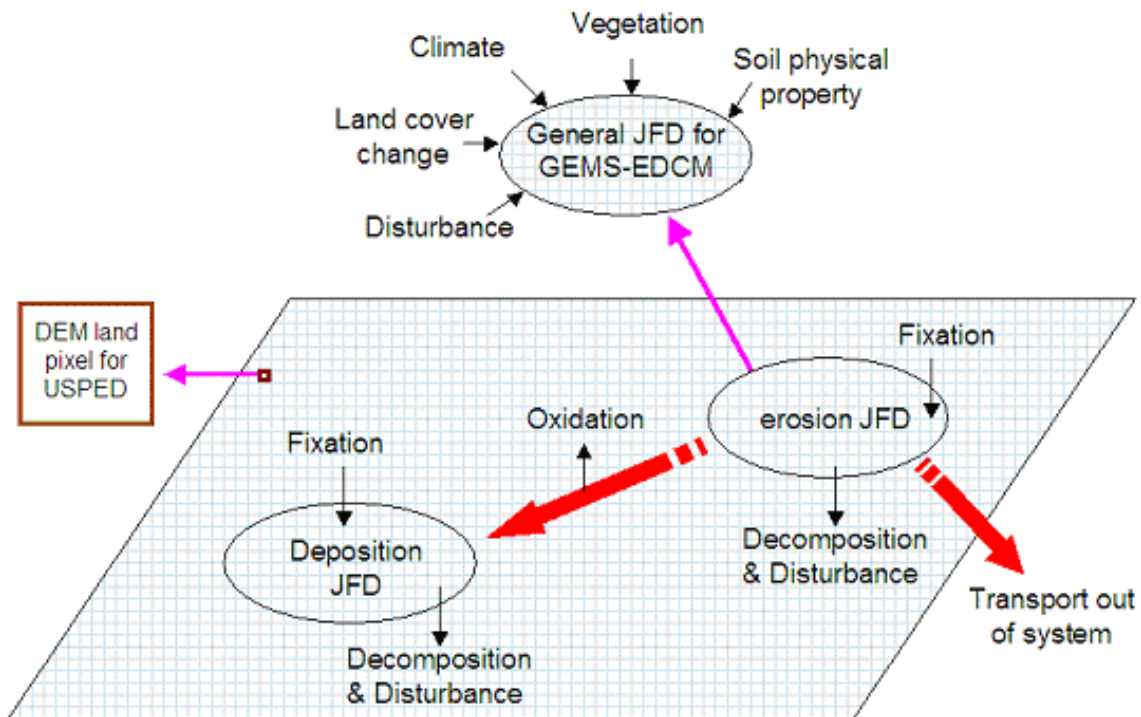


Figure 4. Linking erosion/deposition model with biogeochemical model.

4.2.1.2 Key GEMS Input Data

GEMS is a modeling system that can downscale regional data for use by site level models using a Monte Carlo approach (Liu et al., 2004a). Major input data include the following:

- Spatial GIS coverages of land cover types, climate grid, initial soil profile information (thickness, texture, bulk density, and C and N pools of all soil layers), management and disturbances, and nitrogen deposition map.
- Ecosystem properties such as forest age, crop species, and ecosystem productivity.

- Other fixed (or default) parameter data related to different vegetation type, soil carbon decomposition constants, and lignin contents in plant tissues, etc. Because these parameters can take the default values if no on-site data are available, we will not discuss these data further in this report.

Key spatial data required by GEMS are soils, climate, and land cover changes. The spatial data used to drive GEMS in the US Carbon Trends project (Liu et al., 2004a) is shown in Figure 5.

The model simulations can be performed at the highest spatial resolution of the spatial datasets available for a given region. For example, 60m and 80m resolution length-scales were used in Africa (Liu et al., 2004b) and the US (Liu et al., 2004a), respectively. GEMS can also accommodate a number of soil databases such as the U.S. State Soil Geographic (STATSGO) database and FAO. Other local databases can also be used by GEMS through customized interfaces. Climatic coverages (i.e., monthly precipitation, maximum and minimum air temperatures) can be from different sources. For the United States, GEMS uses the total atmospheric nitrogen deposition from wet and dry sources monitored by the National Atmospheric Deposition Program (<http://nadp.sws.uiuc.edu/>).

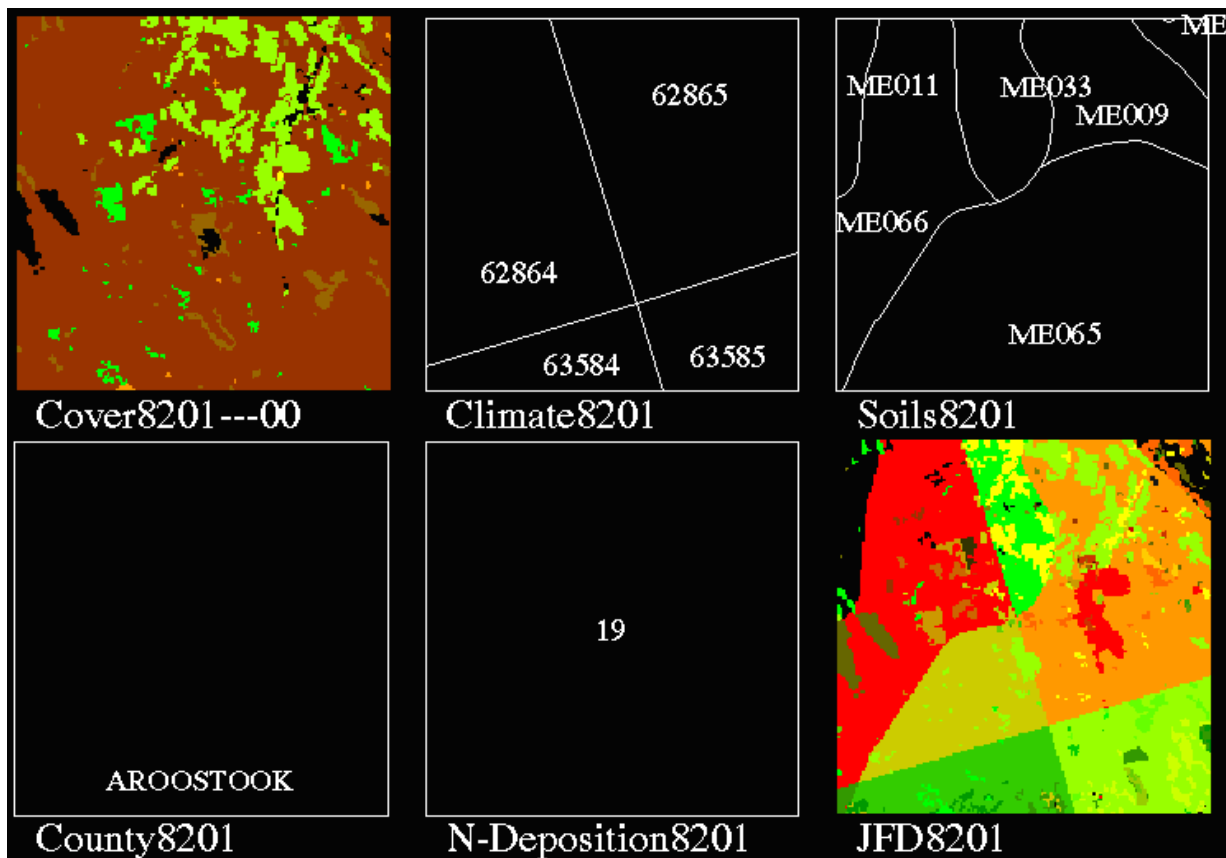


Figure 5. GIS coverages used in GEMS for building simulation units in the US Carbon Trends Project (Liu et al., 2004a). These GIS layers include land cover in

the year 2000, climate polygons, soil map units, county boundary, and nitrogen deposition.

Ecosystem properties data that have been used to support the application of GEMS over large areas include the Forest Inventory and Analysis (FIA) database developed by the U.S. Department of Agriculture (USDA) Forest Service, and the National Resources Inventory (NRI) database developed by the USDA Natural Resources Conservation Service (<http://www.nrcs.usda.gov/tevhncial/NRI>). For example, GEMS uses FIA data to initialize forest age and biomass, and to constrain model simulated forest growth rates (Table 1).

Table 1. Forest age-class and biomass carbon lookup table (unit Mg C ha⁻¹)

Age class	5	15	25	35	45	55	65	75	85	95	105
Area weight (%)	0.17	0.11	0.11	0.13	0.14	0.13	0.09	0.05	0.03	0.02	0.02
C density	9.8	29.8	45.4	55.8	64.6	69.7	79.9	83.8	86.5	89.9	98.8

4.2.1.3 Data for Calibration and Validation

In the US Carbon Trends Project, survey statistics from FIA data (e.g., accumulation of biomass) and agricultural census data (e.g., grain yield), and remotely sensed data (e.g., MODIS NPP) have been used to calibrate and validate GEMS simulations. Other observations can also be used to constrain model simulations. For example, biomass stock change along a chronosequence of forests was used to validate model simulations in Senegal, Africa (Liu et al., 2004b).

4.2.1.4 Other Data

After satisfying the key data requirements, GEMS simulations can be improved if additional data are available. Additional data are not required, but can greatly reduce the uncertainty in model simulations, because models can be better parameterized and better constrained with these additional data. Some limited coding is required if new data types are introduced to GEMS. The following data from Fort Benning might greatly reduce the uncertainty of simulated ecosystem dynamics, carbon and nitrogen cycles, and the impacts of disturbances and management:

- Forest inventory data, including forest age, tree species composition, biomass, growth rates, etc.
- Vegetation mortality and recruitment
- Litter decomposition
- Spatial movement of soil C and N (e.g., erosion and deposition)
- Disturbance history and impact, including fire intensity and frequency, military training type and intensity, logging, etc.

4.2.2 EDCM

EDCM is the embedded ecosystem biogeochemical model in GEMS. It is based on the well-established ecosystem model CENTURY (version IV) (Parton et al., 1993; Liu et al., 2003). The established algorithms of soil organic matter (SOC) dynamics in CENTURY also form the basis of several other biogeochemical models, such as CASA (Potter et al., 1993), InTEC (Chen et al., 2000), and TRIPLEX (Peng et al., 2002). EDCM is capable of simulating C and N dynamics in various ecosystems including forests, crops, pastures, and savannas. Figures 6 and 7 show the C and N pools and fluxes in an agricultural system as simulated by CENTURY and EDCM.

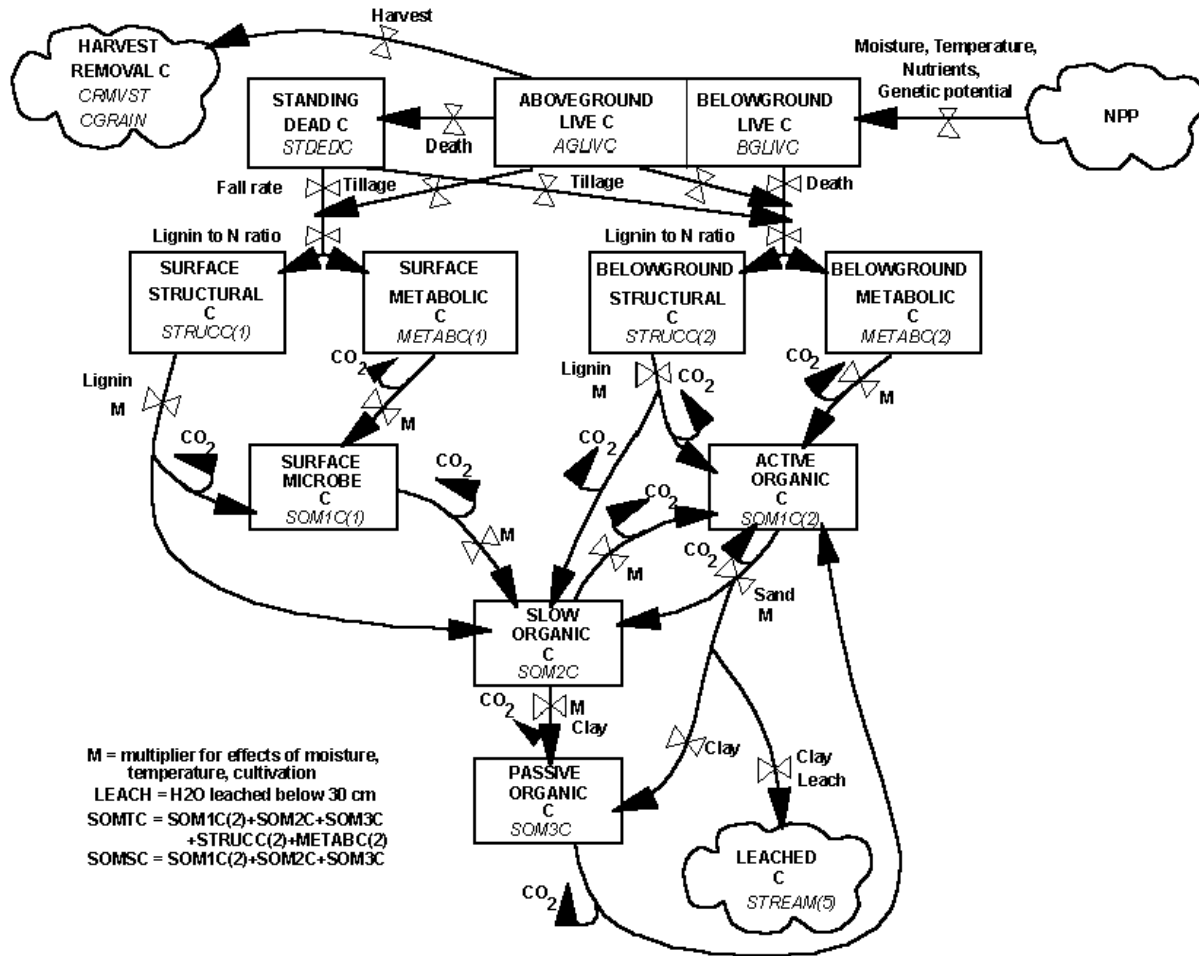


Figure 6. Diagram showing carbon cycling in a terrestrial ecosystem as simulated by the CENTURY and EDCM (Metherell et al. 1993). The algorithms shown here have been well tested worldwide. These established algorithms form the basis of a suite of terrestrial biogeochemical models, including CASA (Potter et al., 1993), InTEC (Chen et al., 2000), TRIPLEX (Peng et al., 2002), EDCM (Liu et al., 2003), and GEMS (Liu et al., 2004a).

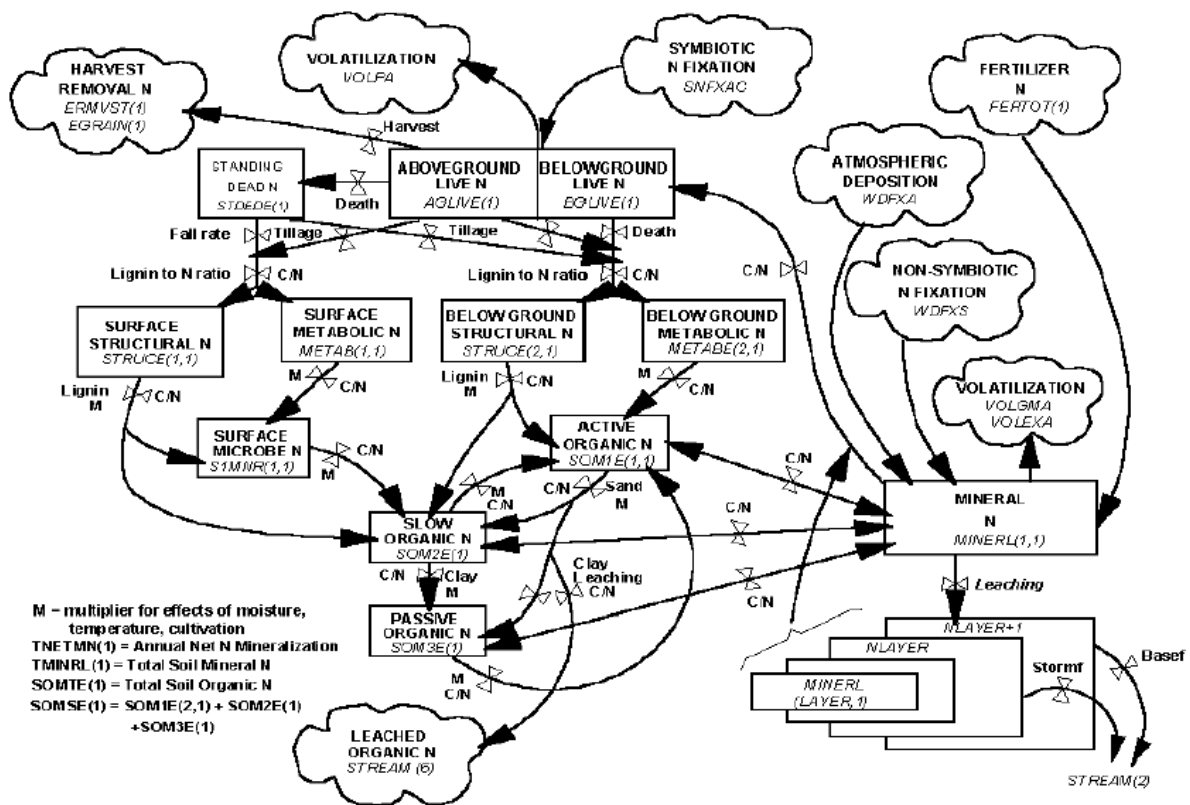


Figure 7. Diagram showing N cycling in a terrestrial ecosystem as simulated by the CENTURY and EDCM (Metherell et al. 1993). It can be seen that the N cycle is tightly coupled with the C cycle (Figure 6).

Owing to its inheritance from its antecedent model CENTURY, EDCM is an advanced biogeochemical models in simulating the impacts of various natural processes (e.g., fires, hurricanes, atmospheric N deposition, atmospheric CO₂ ‘fertilization’, climate change and variability, and erosion and deposition) and management practices (e.g., grain harvesting, timber harvesting, fertilization, land cover and land use change, cultivation, fertilization, and manure addition) on C and N cycles at the ecosystem scale. EDCM can simulate the impact of soil erosion and deposition on C and N dynamics. More than 100 output variables are provided by EDCM, including the net primary production (NPP), net ecosystem production (NEP), C and N stocks in aboveground and belowground biomass, soil carbon dynamics, etc.

CENTURY has a one-soil-layer structure for carbon and nutrients (N, P, and S). In contrast, EDCM adopts a multi-soil-layer structure to account for the stratification of the soil profile and SOC in each soil layer. It dynamically keeps track of the evolution of the soil profile (up to 10 soil layers) and carbon storage as influenced by soil erosion and deposition.

4.2.3 Soil erosion and disturbance representations in GEMS

4.2.3.1 Erosion and Deposition

Many soil erosion and deposition models have been developed during the past few decades. However, not all the models are suitable for the military training installations. Doe et al. (1999) evaluated 24 erosion models against thirteen criteria and identified six models as suitable for applications at military installations. The USPED is one of the suitable models (Figure 11), is based on the unit stream power theory outlined by Moore and Burch (1986). A detailed description is given in Section 4.4.

The USPED are suitable for GEMS and Fort Benning because of its time step, level of complexity, capability of simulating both erosion and deposition, and robustness.

For linking soil C with erosion/deposition, CENTURY 4.0 has a one-soil-layer structure for carbon and nutrients. In contrast, EDCM adopts a multi-soil-layer structure to account for the stratification of the soil profile and SOC in each soil layer. It dynamically keeps track of the evolution of the soil profile (up to 10 soil layers) and carbon storage as influenced by soil erosion and deposition.

In EDCM, each soil C pool in the top layer will lose certain amount of C if erosion happens. The C eroded is calculated as the product of the fraction of top soil layer being eroded, the total amount of SOC in the top 20-cm layer, and an enrichment factor of the eroded SOC. EDCM can dynamically update the soil layers affected by erosion and deposition. But EDCM itself alone is not capable of estimating erosion and deposition.

4.2.3.2 Management and Disturbances

At least we need to consider three types of management practices and disturbances in this study: 1) prescribed fires, 2) military training activities, and 3) forest cutting and planting. These practices and disturbances directly affect vegetation type, biomass stock, soil nutrient level, and soil physical properties. Changes in vegetation and soil properties subsequently influence soil erosion and deposition, vegetation recovery, ecosystem sustainability, wildlife habitat, and future military training activities. The major casual relationships of disturbances to soil and vegetation dynamics are shown in Figure 8.

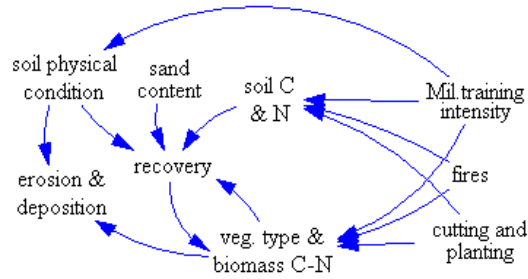


Figure 8. Casual relationships of major disturbances with vegetation and soils in GEMS.

Prescribed fires are often used at Fort Benning to help improving the accessibility of military training areas and restoring the long-leaf pine stands to promote the red-cockaded woodpecker population recovery. Each training compartment is burned from once a year to once every five years.

Military training activities generally lead to the increase of surface soil bulk density (i.e., compaction) and the decrease in soil C and N stocks. Garten and Ashwood (2004a,b) studied the effects of heavy tracked-vehicle disturbance on forest soil properties at Fort Benning. Their results showed that the effects of the bulldozer disturbances were limited primarily to the forest floor (O-horizon) and the surface mineral soil (0–10 cm). Dry mass and C stocks in the O-horizon were significantly reduced by 25 to 75% following one-time disturbance. Bulk density of the surface mineral soil increased by 15%, and soil C and N reduced by 15 to 45%. We will incorporate these experimental results in GEMS. Roads and bare lands are a major source of erosion at military training sites. In the USPED model, we quantify erosion effect using C factor as listed in table 5. Unpaved road and bare land has a C factor of 0.75, which is the second largest value and 150 times larger than that of grass cover and 750 times larger than that of forest cover. Any change in bare land and road leads to changes in erosion.

Forest management at Fort Benning includes thinning of forests (about 2800 ha per year) and clear cutting of unhealthy stands. Fort Benning forest management guidelines require a 100-year harvest rotation for healthy loblolly and shortleaf pine forests. There forest management activities are parameterized in GEMS.

4.2.4 Data Preparation for Model Parameterization

4.2.4.1 Forest Biomass

See section 4.3 for details.

4.2.4.2 Soil Carbon

The spatial database of soils at Fort Benning is obtained from the SERDP Ecosystem Management Program (SEMP) Data Repository. Attributes include soil type, soil organic matter

content, bulk density, etc. The spatial resolution and data formats are equivalent to the Soil Survey Geographic Database (SURRGO) of the National Resources Conservation Service (NRCS), U.S. Department of Agriculture. The soil C calculated from top soil layer (various from 25 to 75 cm in thickness) is averaged at 0.46% by soil weight, roughly 3.5 kg C/m² (Figure 9). Incomplete records were not included in the calculation.

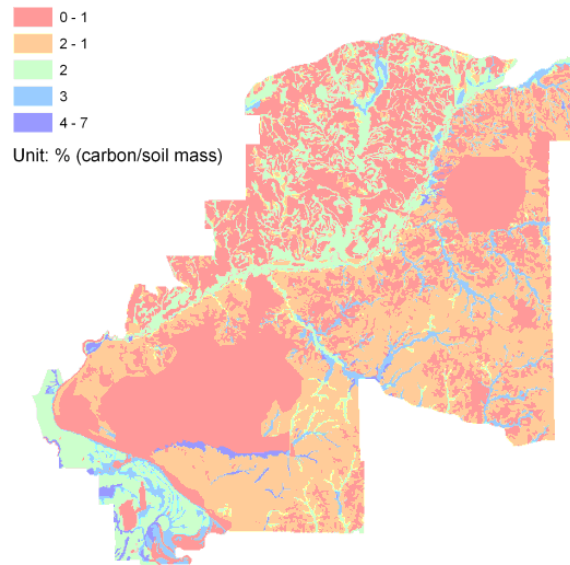


Figure 9. Estimated soil C of top layer (average 25 to 75 cm in thickness) at Fort Benning.

4.2.4.3 Climate

Fort Benning climate data layers have been generated from observations collected from ten meteorological stations (1999–2004) on Fort Benning and nearby National Weather Service stations (Figure 10). The spatial resolution of the data is 1km at a monthly time scale. Experiments with 5km and 0.5km spatial resolution indicated that the 1km resolution was fine enough to retain the spatial details of climate variability.

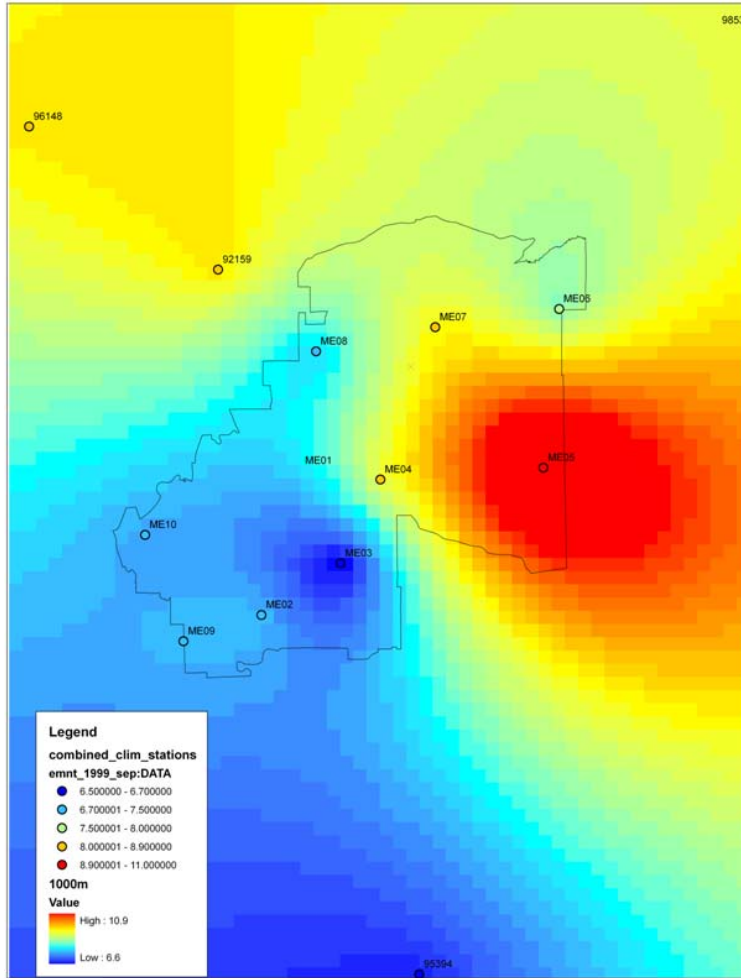


Figure 10. Interpolated 1-km resolution monthly minimum temperature data for Fort Benning. The circles show the weather stations used for interpolation.

4.2.5 Sensitivity Analysis

For a modeling system, a certain amount of change in model parameter value or input data may lead to noticeable changes in model outputs. Because different model parameters and input data have different effects on model outputs, it was necessary to identify the most sensitive parameters and input data. Once identified, special attention was given to the sensitive parameters and key input data in our modeling effort.

The sensitivity of the GEMS to some key input data and parameters was investigated. Table 2 lists the parameter values for the base run.

Table 2. Values for some key inputs/parameters for the base run of the GEMS model.

Input/Parameter	CODE	Value	Unit
Soil bulk density	BULKD	1.37	g/cm ³
Soil sand content	SAND	0.71	%(w/w)
Soil clay content	CLAY	0.04	%(w/w)
Soil silt content	SILT	0.25	%(w/w)
Total soil carbon	SOMTC	1915	g/m ²
Surface active soil carbon	SOM1	61	g/m ²
C:N of slow soil organic matter	C:NSOM2	16.2	--
C:N of passive soil organic matter	C:NSOM3	9.6	--
Leaf biomass	LEAFC	71.3	g/m ²
Decomposition rate of dead branch	DECW1	8	year ⁻¹
NPP allocation ratio to leaf	LEAFFR	0.4	%(w/w)
Forest age	AGE	22	year
Maximum potential NPP	PRDX4	220	g C /m ² /yr

Table 3 shows the sensitivities of four key variables in the carbon cycle: the simulated NPP, forest biomass carbon (FRSTC), soil organic carbon in the top 20-cm layer (SOMTC), and total ecosystem carbon (FSYSC = FRSTC + SOMTC) to the changes of these parameters (using 90% and 110% of the base parameter values).

Table 3. GEMS model sensitivity to key inputs/parameters. Values indicate relative change (%) to the reference run.

	NPP		total ecosystem carbon		soil organic carbon		forest biomass carbon	
	90% test	110% test	90% test	110% test	90% test	110% test	90% test	110% test
bulkD	0.3	-0.7	0.1	-0.2	-0.1	0.0	0.2	-0.3
sand	-2.1	1.6	-0.4	0.2	0.9	-1.0	-0.8	0.6
clay	0.0	0.0	0.0	0.0	0.0	0.0	0.0	0.0
silt	-0.3	0.2	-0.1	0.1	0.0	-0.1	-0.2	0.1
somtc	-4.6	4.4	-3.2	3.1	-7.4	7.4	-1.6	1.5
som1	-0.5	0.5	-0.2	0.2	-0.3	0.3	-0.2	0.2
C:Nsom2	5.1	-4.4	2.0	-1.7	1.8	-1.6	1.8	-1.6
C:Nsom3	0.1	-0.1	0.0	0.0	0.0	0.0	0.0	0.0
leafC	-0.4	0.4	-0.3	0.3	-0.3	0.3	-0.3	0.2
decw1	0.0	0.0	0.0	0.0	-0.1	0.1	0.0	0.0
leafC	0.3	-1.4	-0.3	-0.2	0.9	-1.4	-0.5	0.3
age	0.1	0.0	0.1	-0.1	-0.1	0.2	0.1	-0.2
PRDX4	-12.1	5.2	-6.5	3.0	-6.3	2.7	-6.1	2.9
reference	0.0	0.0	0.0	0.0	0.0	0.0	0.0	0.0

Figure 11 is the graphic display of NPP sensitivity. Sensitivity analysis showed that: Estimated NPP, total ecosystem C, total initial soil organic C, and aboveground forest biomass C are very

sensitive to the PRDX4 parameter, an empirical maximum potential gross primary production variable for the model system. Except for biomass C, the other three outputs were significantly affected by the initial level of the soil organic C. The four model outputs were moderately sensitive to the C:N ratio of the slow soil organic C pool (C:NSOM2), and the sensitivity of the four outputs to C:NSOM2 is negative, which was different from their sensitivity to other parameters. These four major output variables were not sensitive to other parameters investigated.

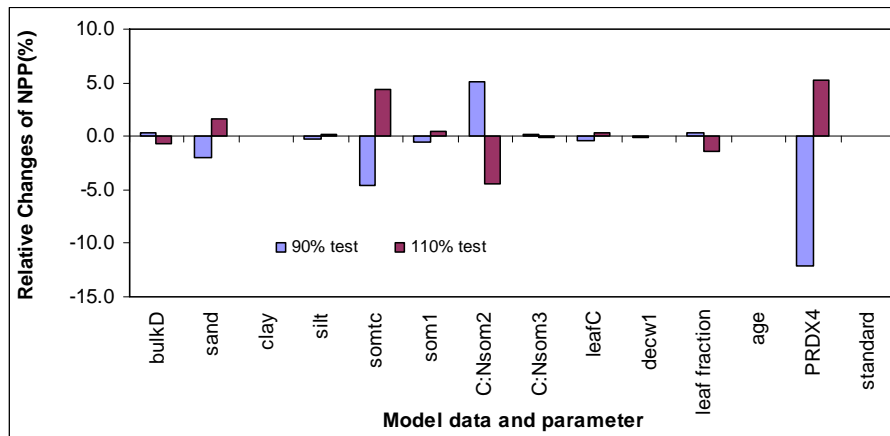


Figure 11. GEMS NPP sensitivity to model parameters.

4.3 Fort Benning Forest States and Trends

Two inventory datasets were used to characterize forest status and trends. Current inventory data (including inventories from 2006 to June 2007) containing detailed records of diameter at breast height (DBH), height, and total basal area (BA) for each tallied tree, covered a small portion of the forest stands (186 km², 25% of the Fort Benning area) (Figure 12). In contrast, the historical inventory data covered more stands (636 km², 86% of Fort Benning area) that were inventoried from 1981 to 2000. However, it contained only stand basal area with no information on tree DBH and height. Therefore the two major issues in forest inventory are: (1) long inventory interval and less comparable stands, (2) some inconstant measurements. In terms of carbon accounting, one major uncertainty comes from the representation of forest age and biomass change after disturbances. For example, selective cutting could increase or decrease forest stand age hence affecting forest growth. What is more, in current GEMS, the modeled selective cutting is an average area ratio and therefore brings uncertainty estimates when compared to location-specific observations. As for fire, fire induced biomass loss and mortality rate change could greatly impacts carbon and nitrogen cycle. Our suggestion for future forest inventory include: First, consider establishing a limited number of forest field plots that can be re-measured at an interval of less than 5 years. The forest stand change is best analyzed when such continuous measurements are available. Second, key variables of forest stand should be monitored consistently, including tree height, DBH, density, canopy cover, dead wood, ground litter stock, major management/disturbance events, and biomass removed by management and natural

disturbance etc. Third, any ground measurements that helps to calibrate remote sensing observations should also be considered.

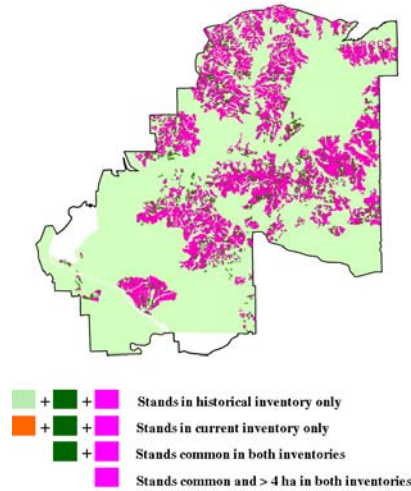


Figure 12. The spatial extents of the current and historical forest inventories.

Total aboveground and belowground biomass carbon of each tallied tree (agbc and bgbc, kg C/tree) in the current inventory was estimated using the equations from Brown et al. (1997) and Cairns et al. (1997). The biomass of midstory (DBH<5 inches) and understory was not estimated. To estimate biomass from stand BA in the historical database, a relationship between stand BA and stand biomass was developed from the current dataset (Figure 13). Forest change was assessed using forest stands that were inventoried both in the current and historical databases. We focused on the stands larger than 4 ha (pink area in Figure 16), the minimum area of a stand used in the inventories.

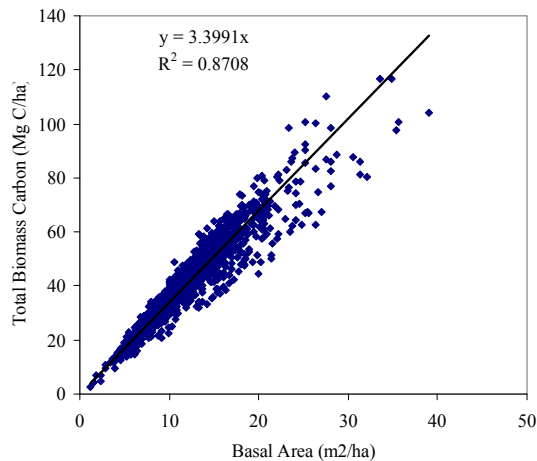


Figure 13. Relationship between stand basal area and total stand carbon density based on the current inventory.

4.4 Estimating Soil Erosion and Deposition

4.4.1 USPED

The algorithm for the simulation of soil erosion in USPED is similar to that of the USLE or RUSLE model. However, there is a fundamental difference between these two models. USLE or RUSLE assumes that erosion mainly depends on rainfall detachment capacity, while USPED assumes that soil erosion depends on not only rainfall detachment capacity, but also the sediment transport capacity of the surface runoff. In some cases, erosion does not occur in USPED even if soil particles are detached by the kinetic energy of rainfall because of the limitation of sediment transport capacity of surface runoff. Sediment transport capacity is a function of runoff amount, terrain characteristics, and surface roughness and friction. If the transport capacity is exceeded by the sediment loading at a given location, deposition would happen in USPED. The amount of deposition is the difference between sediment load and the transport capacity.

In USPED, the sediment flow rate $qs(r)$ (where $r=(x,y)$ is the pixel location in the DEM), assumed to be at the sediment transport capacity $T(r)$ when transport capacity is limiting, is approximated by

$$qs(r) = T(r) = K_t(r) |q(r)|^m \sin b(r)^n \quad (1)$$

where $b(r)$ [deg] is slope, $q(r)$ is water flow rate, $K_t(r)$ is transportability coefficient dependent on soil and cover, m and n are constants depending on the type of flow and soil properties. For overland flow, the constants are usually set to $m=1.6$, $n=1.3$.

Accurate estimation of the spatial dynamics of flow rate on landscape is challenging and data-demanding, if not impossible. In practice, the calculation of sediment transport capacity T in USPED is approximated using the assumption of steady state water flow. Steady state water flow can be expressed as a function of upslope contributing area per unit contour width $A(r)$

$$|q(r)| = A(r)i \quad (2)$$

where i is uniform rainfall intensity. Note that this approximation by upslope area neglects the change in flow velocity due to cover. For the uniform soil and cover properties represented by $K_t = \text{const}$.

The masses of water and sediments are conserved in USPED through continuous 2-dimensional horizontal routing in space. The water and sediment flows may vary across land pixels because of the influence of local terrain features and other land surface conditions. The net flow change on a 2-dimensional plane indicates whether a given land pixel acts as a sink or a source of the materials (i.e., water and/or soils). Thus, the net erosion/deposition rate (ED) within a land pixel can be calculated as a divergence of the sediment flow (see Appendix in Mitás and Mitásova, 1998):

$$ED = \text{div}(T) = K_r \{ \text{grad}(h) \cdot s \cdot \sin(b) - h(k_p + k_r) \} \quad (3)$$

where s is the unit vector in the steepest slope direction; h is water depth; k_p is the profile curvature, and k_t is the tangential curvature. ED can be positive (deposition), negative (erosion), or zero (no erosion or deposition).

According to the 2D formulation (equation 3), the spatial distribution of erosion and deposition is controlled by the change in the overland flow depth (first term) and by the local geometry of terrain (second term), including both profile and tangential curvatures. The bivariate formulation thus demonstrates that the local acceleration of flow in both the gradient and tangential directions (related to the profile and tangential curvatures) play equally important roles in spatial distribution of erosion/deposition. The interplay between the magnitude of water flow change and both terrain curvatures reflected in the bivariate formulation determines whether erosion or deposition occurred.

Because no experimental work was originally performed to develop parameters needed for USPED by USPED developers, the USLE or RUSLE parameters were used to represent the impacts of soil and cover through a matching process. The RUSLE equation is:

$$E = R \cdot K \cdot LS \cdot C \cdot P \quad (4)$$

where E is estimated average soil loss, R is rainfall-runoff erosivity factor, K is soil erodibility factor, L is slope length factor, S is slope steepness factor, C is cover management factor, and P is support practice factor.

Assuming that sediment flow at sediment transport capacity can be estimated as

$$T = R \cdot K \cdot P \cdot A(r) \cdot (\sin b)^n \quad (5)$$

The net erosion/deposition is estimated as (Mitasova, 1998):

$$ED = \text{div}(T \cdot s) = d(T \cdot \cos \alpha) / dx + d(T \cdot \sin \alpha) / dy \quad (6)$$

where α [deg] is aspect of the terrain surface, $dx = dy$ is the grid resolution, $KCP \sim K_t$ and $LS = A(r) (\sin b)^n$, and $m=1.6$, $n=1.3$ for prevailing rill erosion while $m=n=1$ for prevailing sheet erosion. This equation is equivalent to the relationship with curvatures presented above (equation 2). However, the computational procedure is much simpler. It should be noted that USPED in the forms of x and y was to obtain a relative rather than absolute estimate of net erosion and deposition. Caution should be used when interpreting the results because the USLE parameters were developed for simple plane fields and detachment limited erosion therefore to obtain accurate quantitative predictions for complex terrain conditions they need to be re-calibrated (Mitasova et al., 1996).

We followed the general procedures for calculating erosion and deposition outlined at the USPED web site (<http://skagit.meas.ncsu.edu/~helena/gmslab>). In the following, we describe our methodology for determining the parameters of USPED at Fort Benning.

4.4.2 Determination of USPED Parameters at Fort Benning

4.4.2.1 Flow Accumulation

One common simplification in estimating the flow accumulation is to assume that the land pixels of upslope contributing areas contribute equally to surface run-off. This might be convenient in calculation. However, it ignores the fact that the upslope area may be composed of different land cover types (i.e., forest, grassland, or bare land) combined with different soil types, and each contributes differently to surface runoff generation. The cumulative run-off amount (i.e., flow accumulation) directly affects sediment transport capacity, hence influencing erosion and deposition. Therefore, it is important to incorporate the impacts of spatial variation of soil and vegetation into the calculation of flow accumulation. In this study, we used the normalized USDA NRCS runoff curve numbers to weight the calculation of flow accumulation.

The runoff curve number (CN) is an empirical parameter used for predicting direct runoff from rainfall excess. The runoff curve numbers for characteristic land cover descriptions and hydrologic soil groups were derived from an empirical analysis of runoff from small catchments and hillslope plots monitored by the USDA. The curve number has a range from 30 to 100 with lower numbers indicating low runoff potential and larger numbers for higher runoff potential.

To account for the impacts of land cover types and hydrological soil groups on surface runoff generation, we first generated a series of runoff curve number maps using dynamic land cover maps and a static hydrological soil group map. The runoff curve number maps were normalized to 0.3 to 1.0 by dividing these maps by 100. These normalized maps were then used as the weight for calculation flow accumulation using FLOWACCUMULATION in ArcGIS. With the curve-number weighting factor, the flow accumulation calculated for a given pixel contains various contributions from multiple upslope pixels. Soils at Fort Benning are classified into four hydrological soil groups according to SCS (1986):

- Group A: High infiltration (low runoff). Sand, loamy sand, or sandy loam.
- Group B: Moderate infiltration (moderate runoff). Silt loam or loam.
- Group C: Low infiltration (moderate to high runoff). Sandy clay loam.
- Group D: Very low infiltration (high runoff). Clay loam, silty clay loam, sandy clay, silty clay, or clay.

These hydrological soil groups were then used in combination with land cover classes to determine the runoff curve numbers according to the guidelines provided in SCS (1986). The representative curve numbers for Fort Benning are listed in Table 4. Most of the bare grounds at Fort Benning were created by maneuvering tracked and wheeled vehicles and the curve numbers for dirt roads from SCS (1986) were assigned to these bare grounds. The curve numbers of this cover class were also very similar to the values of the cultivated agricultural lands without

conservation treatment (no terraces). The curve numbers for herbaceous land cover class were calculated as the averages of the curve numbers assigned to poor (<50% ground cover) and good (50–70% ground cover) by SCS. The ground cover conditions of pine forests were considered to be fair because of the frequent prescribed understory burning. On the other hand, the ground cover of hardwoods, lacking prescribed burning, was considered to be good. Apparently, the impacts of military training impacts (e.g., dramatic changes in land cover) and ecosystem management practices (e.g., prescribed burning) were incorporated into the determination of the curve numbers in Table 4.

The empirical relationship between CN and land cover type indicates the relative production of surface runoff, which is the key driver of soil erosion and deposition. Bare land and unimproved road have a larger CN value (72) than vegetated cover (30~59), meaning higher runoff water production. In USPED model, the modified flow accumulation calculation with CN combines C,K,P, to calculate soil erosion and deposition.

Table 4. Table of Runoff Curve Numbers.

Land Use	Hydrologic Soil Group			
	A	B	C	D
Paved Roads	98	98	98	98
Urban	98	98	98	98
Bare ground and unimproved road	72	82	87	89
Herbaceous (50% cover)	59	70	80	85
Scrub and shrub	45	66	77	83
Pine forests	36	60	73	79
Mixed forests and hardwoods	30	55	70	77
Water	100	100	100	100

4.4.2.2 The C Factor

The C factor, or cropping factor, represents the effect plants, soil cover, soil biomass, and soil disturbing activities have on erosion. It is the most complicated of the USLE factors. It incorporates effects of tillage, crop type, cropping history, and crop yield. Cropping factors for forested, agricultural, and urban lands were provided by the Georgia Forestry Commission (GFC), Natural Resources Conservation Service (NRCS), and U.S. Environmental Protection Agency (EPA), respectively. The assigned C-factors values for the different land cover classes were obtained from literature. C-factor values for the same land cover types vary depending on the geographical location of the area. In order to obtain best possible results, data from similar geographical settings were chosen (Table 5).

Table 5. C-factor values for Fort Benning land cover types.

land cover type	C factor	Source/Notes
water	1.000	No erosion from water but deposition can happen
evergreen(planted)	0.001	NRCS value for Georgia
evergreen	0.001	ditto
hardwood	0.001	ditto

shrub	0.005	Draft EPA report
herb	0.003	Draft EPA report
bare land	0.750	draft EPA report (similar to mining)
mixed forest	0.001	NRCS value for Georgia
unpaved road	0.750	Draft EPA report
urban	0.003	Jackson et al., 2005; Draft EPA report

4.4.2.3 The R factor

The long-term mean R factor was mapped for the contiguous United States, and ranged from 20 to 550. For Fort Benning, Georgia, the long term mean R was 350. When estimating annual variation of erosion and deposition, the R factor should be adjusted according to annual rainfall. In our USPED application, we used annual rainfall to modify the average R factor to obtain the possible effects of climate variation:

$$R_u = \frac{P}{P_0} R \quad (7)$$

where R_u is the modified R factor, P_0 is the long-term average rainfall, and P is the actual rainfall of an individual year.

4.4.2.4 The K Factor

The soil erodibility factor is determined experimentally for a given soil type and is reported by the National Soil Conservation Service (NRCS). The values for the K factor across Fort Benning were provided in its soil spatial database. The resolution of the soil database was equivalent to that of the USDA Soil Survey Geographic (SSURGO) database.

4.4.3 Model Testing

To evaluate impacts of military disturbances on erosion and deposition, ten watersheds representing a range of disturbances, soil types, topography, and land cover classes were monitored (Houser et al., 2006). To evaluate the performance of USPED in simulating soil erosion and deposition at Fort Benning, simulated net erosion and deposition at the monitoring positions were compared with total suspended solids in runoff generated from these catchments.

4.5 Simulating Impacts of Cyclic Prescribed Fire on Ecosystem C and N Cycles

4.5.1 The EDCM Model and Parameterization

EDCM is an ecosystem model capable of simulating C and N cycles in various ecosystems under the impacts of management practices, disturbances, and climate change (Figure 14). For details on the model description, see Liu et al. (2003).

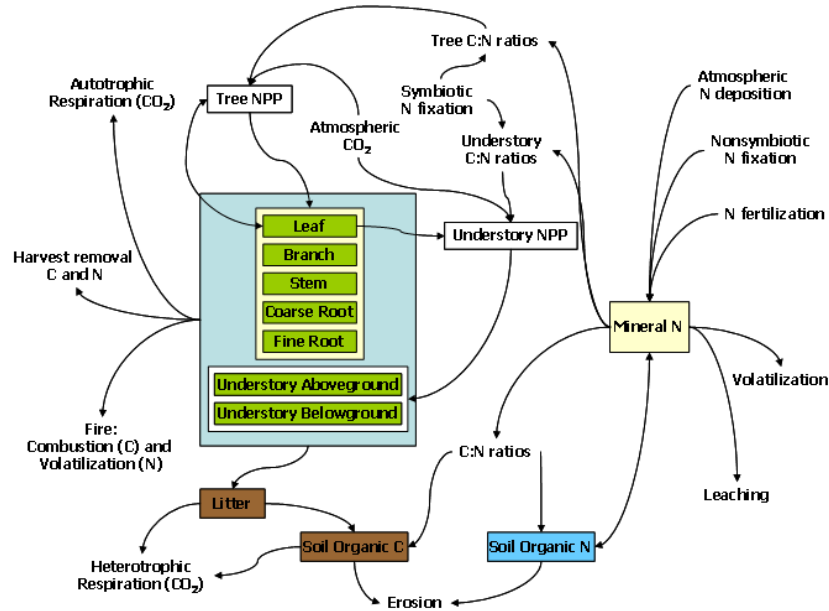


Figure 14. Major C and N cycling processes and pools in the Erosion-Deposition-Carbon Model (EDCM).

In EDCM, the impacts of prescribed fire on C and N cycles are simulated using a canopy woody layer and an understory layer, and fire removal of forest floor (litter) and understory aboveground are coupled. Certain fractions of litter and understory aboveground biomass and nutrients are consumed by fire according to burning intensity. All simulated fires occur in the dormant season during the 200-year period. N_2 fixation, expressed as g N fixed per g C fixed, can occur in both layers. N competition between the canopy and understory is largely controlled by the canopy coverage. In this study, we simulated C and N cycles at relatively infertile longleaf pine sites at Fort Benning. Key model parameters, including C: N ratios of plant tissues, soil, atmospheric N deposition rate, symbiotic and nonsymbiotic N_2 fixation, and C allocations among plant parts were either measured from previous studies (DeBusk et al., 2005; Garten and Ashwood, 2004a) or taken from literature review (DiStefano and Gholz, 1989; Hendricks and Boring, 1999; Lajeunesse et al.; 2006). Meteorological data (monthly precipitation and temperature) were from on-installation weather stations. Forest biomass C and soil organic C stocks were estimated based on forest inventory and Soil Survey Geographic (SSURGO) database for Fort Benning.

4.5.2 Modeling Experimental Design and Analysis

Four levels of fire frequency, fire intensity, symbiotic N_2 fixation, and nonsymbiotic N_2 fixation were used to encompass their variability in the study area, and their combinations were used to assess the impacts of cyclic prescribed burning on C and N dynamics (Table 6). Atmospheric N deposition of $0.35 \text{ g N/m}^2/\text{yr}$ was used for all model simulations. Combinations of fire frequency, fire intensity, and symbiotic and nonsymbiotic N inputs were generated using factorial experimental design (PROC FACTEX; SAS, 2004). Excluding the unrealistic combinations

(e.g., fire frequency is 0 years with intensity of low, intermediate, and high), a total of 160 scenarios were generated. It should be recognized that the fire intensity levels used in our study was relative to the amount of aboveground live and dead biomass consumed by fire. These levels might not necessarily correspond to the intensity measures used in the field by the fire crew.

Table 6. Experimental design for the combinations of fire frequency, fire intensity, and symbiotic and nonsymbiotic N inputs.

	No	Low	Intermediate	High
Fire Frequency	0	5 yrs return interval	3 yrs return interval	1 yr return interval
Fire intensity	0	Consume 40% of understory aboveground, and 30% of litter	Consume 70% of understory aboveground, and 60% of litter	Consume 95% of understory aboveground, and 90% of litter
Symbiotic N ₂ fixation rate (g N/m ² /yr)	0	0.03 ^a	0.35	0.7 ^b
Nonsymbiotic N ₂ fixation rate (g N/m ² /yr)	0	0.1 ^c	0.3 ^c	0.5 ^c

a Lajeunesse et al. (2006)

b Hendricks and Boring (1999)

c DiStefano and Gholz (1989)

Impacts of different factors on simulated C and N fluxes and stocks were analyzed using multivariate canonical regressions (PROC CANCORR; SAS, 2004). Because it is difficult to comparatively visualize all 160 simulated scenarios, we averaged and presented the results according to treatment levels. The significance of treatment differences was determined using ANOVA (PROC GLM; SAS, 2004) with $\alpha \leq 0.05$. In addition, we provided the detailed results of four scenarios (Table 7) to analyze long-term impacts of fire. The major criterion for the selection of these scenarios was to provide feasible options for future fire management at Fort Benning. High frequency or low intensity fire regime is not economic efficiency, so we did not consider the scenarios with high frequency or low intensity. The effect size of fire on C and N dynamics was measured by strength and steepness of change over time. The strength was reflected by the square of the correlation coefficient (r^2). The steepness, reflected by the slope (b), was used to indicate how rapidly C and N fluxes and stocks change over time.

Table 7. Four scenarios for detailed analysis of C and N dynamics. The specifications of low, intermediate, and high are listed in Table 8.

Scenario Code	Fire frequency	Fire intensity	Symbiotic fixation	N	Nonsymbiotic fixation	N
1333	Low	High	High		High	
2333	Intermediate	High	High		High	
2222	Intermediate	Intermediate	Intermediate		Intermediate	
2311	Intermediate	High	Low		Low	

We assumed that the scenario with the combination of intermediate fire frequency, high intensity, low levels of symbiotic and nonsymbiotic N₂ fixation is the current fire regime and biological N input scenario (i.e., the control simulation). Major evidence includes approximately a 3-year return interval for prescribed fire and low biological N₂ fixation inputs in the Fort Benning ecosystems (e.g., Garten and Ashwood, 2004b; Lajeunesse et al., 2006).

4.6 Differences in Carbon Sequestration between Fort Benning and Surrounding Areas

Four counties, Muscogee, Marion, Chattahoochee and Russell, were selected to compare with Fort Benning. This is because these counties surround the Fort Benning installation and have very different land cover management from that of the Fort Benning. In addition, county map is one of the layers used in GEMS. Soil data are also collected based on county tertiary. For GEMS model results, we used 1992–2007 as “current” because the forest inventory data of this period were employed as ground truth. Because carbon sequestration (flux) is quite variable between years due to climate and disturbances, we choose to use the average flux value between 1992 and 2007 as a reference carbon sequestration level. For 2008–2050, because the all the land cover change and climate change are scenarios, we simply average them to represent future condition.

4.6.1 LUCC Databases

Consistent, high-quality, and spatially explicit LUCC databases at 250m × 250m resolution were developed using the FOREcasting SCEnarios of future land cover (FORE-SCE) model (Sohl et al., 2007). FORE-SCE projects future land use changes based on historical land cover change trends, spatial characteristics of recent land cover change, and probability-of-occurrence surfaces for each unique land cover type. FORE-SCE relies heavily on USGS Land Cover Trends data (Loveland et al., 2002) for model parameterization. We extrapolated Land Cover Trends results from the 1992 to 2000 time period, providing ecoregion-by-ecoregion annual “prescriptions” for key variables (e.g., the rates of change for individual land cover types, likelihood of specific land cover transitions, and basic characteristics of patch size) required by FORE-SCE. Logistic regression was used to develop probability-of-occurrence surfaces for each land cover type based on biophysical and socioeconomic drivers related to land use type at a given location. Individual patches of new land cover were placed on the landscape in an iterative process until the annual scenario prescriptions had been met. Patch sizes were uniquely assigned to each new patch by approximating the historical distribution of patch sizes for each land cover type. The process continues with yearly iterations, with a history variable tracking age classes for forest and other classes. A more detailed description of the model is found in Sohl and Saylor (2008).

4.6.2 Other Data Sources

Monthly minimum and maximum temperatures and precipitation were obtained from the Parameter-elevation Regressions on Independent Slopes Model (PRISM) group (1992–2007) and the World Climate Research Programme's (WCRP's) Coupled Model Intercomparison Project phase 3 (CMIP3) A1B (business as usual) scenario (2008–2050). Initial soil properties were based on the Soil Survey Geographic (SSURGO) Database

(<http://soils.usda.gov/survey/geography/ssurgo/>). Soil properties used included soil texture (sand, silt, and clay fractions), bulk density, organic matter content, wilting point, and field capacity. Soil drainage classes from excessively well drained to very poorly drained were indicated by the Compound Topographic Wetness Index (<http://edna.usgs.gov/Edna/datalayers/cti.asp>). Forest species composition, forest age, and biomass distribution data at the county level were obtained from the Forest Inventory and Analysis National Program (<http://fia.fs.fed.us/tools-data/default.asp>). Initial data for the Georgia counties were inventoried in 1989, and data for the Alabama county were inventoried in 1990. Cropping practices, including shares of various crops and rotation probabilities, were derived from the National Resources Inventory (NRI) database, developed by the Natural Resources Conservation Service, US Department of Agriculture (<http://www.nrcs.usda.gov/technical/NRI/>). Total atmospheric nitrogen deposition from wet and dry sources was obtained from the National Atmospheric Deposition Program (<http://nadp.sws.uiuc.edu/>).

4.6.3 Model Simulations

GEMS was developed to upscale carbon stocks and fluxes from sites to regions with a spatially explicit, dynamic consideration of LUCC information (Liu et al., 2004a, 2004b; Liu, in press; Tan et al., 2005, 2006, 2007). GEMS consists of three major components: one (or multiple) encapsulated ecosystem biogeochemical model, an automated model parameterization system (AMPS), and an input/output processor (IOP). The plot-scale Erosion-Deposition-Carbon Model serves as the encapsulated ecosystem biogeochemical model in GEMS (Liu et al., 2003). The spatial deployment of the site-scale model in GEMS is based on the spatial and temporal joint frequency distribution (JFD) of major driving variables (e.g., land use and land cover change, climate, soils, disturbances, and management). The JFD was generated by overlaying these geospatial data layers with a common grid size of 250m by 250m. Model simulation units were the unique combinations of these data layers with the finest simulation unit being one grid cell (i.e., 250m by 250m). The uncertainties of data layers at coarser resolutions were incorporated into GEMS simulations via a Monte Carlo approach. This approach embedded in GEMS maximally uses the finest information contained in some data layers (LUCC data in this study, for example), and other coarser resolution data layers are scaled down to the finest resolution through representation of uncertainty. A more detailed description of the model can be found in Liu et al. (2004a) and Liu (in press).

We developed a data assimilation approach to inversely calculate spatially explicit model parameters from Moderate Resolution Imaging Spectroradiometer (MODIS) net primary production (NPP). The averages of MODIS NPP between 2000 and 2004 were used for inversion. These spatially explicit model parameters were then used to predict NPP. We used 2005 MODIS NPP for model validation. It can be seen that model simulations were in good agreement with MODIS NPP (Figure 15).

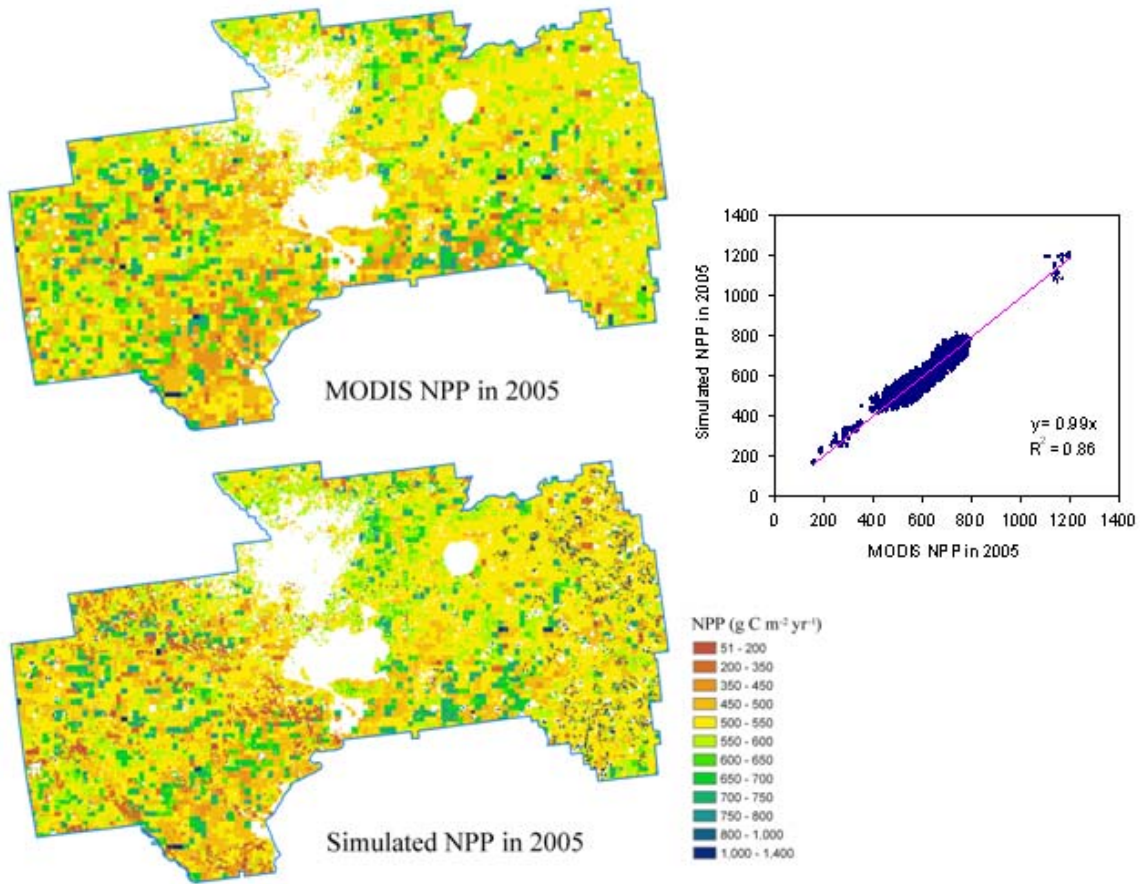


Figure 15. Comparison of GEMS NPP (Y) and MODIS NPP (X) in 2005 ($Y=0.99X$, $R^2=0.86$, $n=43166$).

4.6.4 Analysis

Carbon sequestration was calculated by the difference between current year's and previous year's ecosystem carbon stock, which was equal to net biome productivity (NBP) using the carbon cycle concepts and terminology of Chapin et al. (2006). Ecosystem carbon sequestration included the amount of net carbon accrued in live biomass, the forest floor, and the soil. Positive values represent uptake, and negative values indicate carbon loss from the biome. All the fluxes (e.g., grain yield, wood harvest, and carbon sequestration) were calculated on the basis of total land area in the region. To compare ecosystem carbon dynamics between Fort Benning and surrounding areas, we calculated the carbon sequestration at Fort Benning and surrounding areas.

Section 5 Results and accomplishments

5.1 Fort Benning Forest Status and Trends

A total of 42 tree species were tallied in the current inventory. Table 8 lists the species that accounted for more than 0.5 percent of the total biomass carbon. Loblolly pine (*Pinus taeda*) accounted for about half of the basal area (BA), biomass, and number of trees. Longleaf pine (*P. palustris*) accounted for 23 percent of the total BA and biomass carbon, but only about 17 percent of the total number of trees; this suggests that the individuals of longleaf pine trees were larger than others on average. Nevertheless, the current inventory did not reflect the overall conditions of forests at Fort Benning because the focus was on pine and mixed forests.

Table 8. Basal area, biomass carbon, and number of trees by dominant species (total biomass C share >0.5 percent) at Fort Benning around 2006.

Species	Basal Area m ²	%	Total Biomass C Mg (10 ⁶ g)	%	Number of trees	% of trees
Blackjack Oak	1979	0.9	6113	0.7	47379	1.2
Black & Tupelo Gum	1690	0.7	5582	0.7	34542	0.9
Hickory	3581	1.5	12292	1.5	64542	1.6
Laurel Oak	3176	1.4	10906	1.3	58248	1.5
Loblolly Pine	113065	48.6	398429	48.7	1945109	49.0
Longleaf Pine	52280	22.5	195578	23.9	665426	16.8
Post Pine	4975	2.1	15742	1.9	115247	2.9
Shortleaf Pine	16691	7.2	55114	6.7	357515	9.0
Slash Pine	5016	2.2	16367	2.0	100674	2.5
Southern Red Oak	8074	3.5	29900	3.7	113934	2.9
Sweetgum	7376	3.2	23635	2.9	167087	4.2
Water Oak	7631	3.3	25501	3.1	150120	3.8
Yellow Poplar	1261	0.5	4043	0.6	14894	0.4
Total	232437		817978		3967385	

Stand tree density (current), age (historical), and total biomass carbon (historical) are shown in Figures 16–18, respectively. Most forest stands were younger than 80 years old, and had total biomass carbon less than 80 Mg/ha.

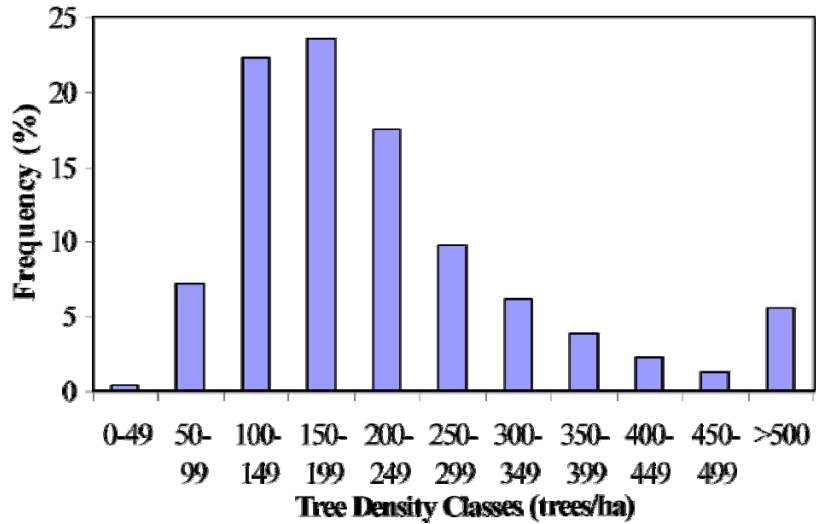


Figure 16. Distribution of tree density of Fort Benning forests around 2006. Tree density varied from 15 to 1,347 trees/ha across all the stands around 2006 with an average of 204 trees/ha.

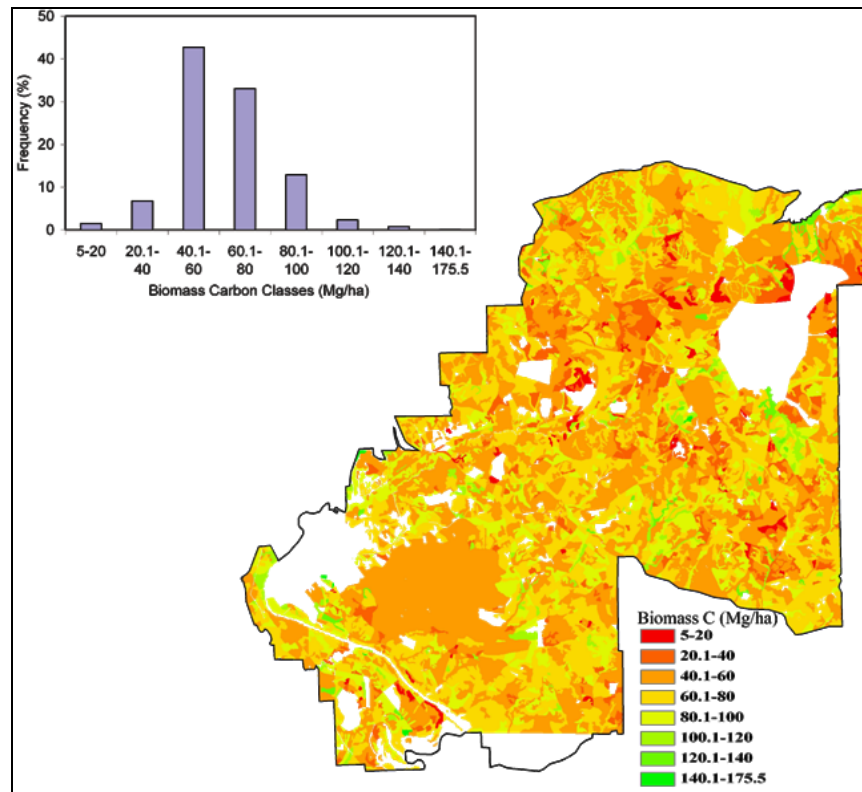


Figure 17. Fort Benning forest age distribution according to the historical inventory. The youngest and oldest forests stands in the database were 1 and 332 years old, respectively, with an average age of 61 years old.

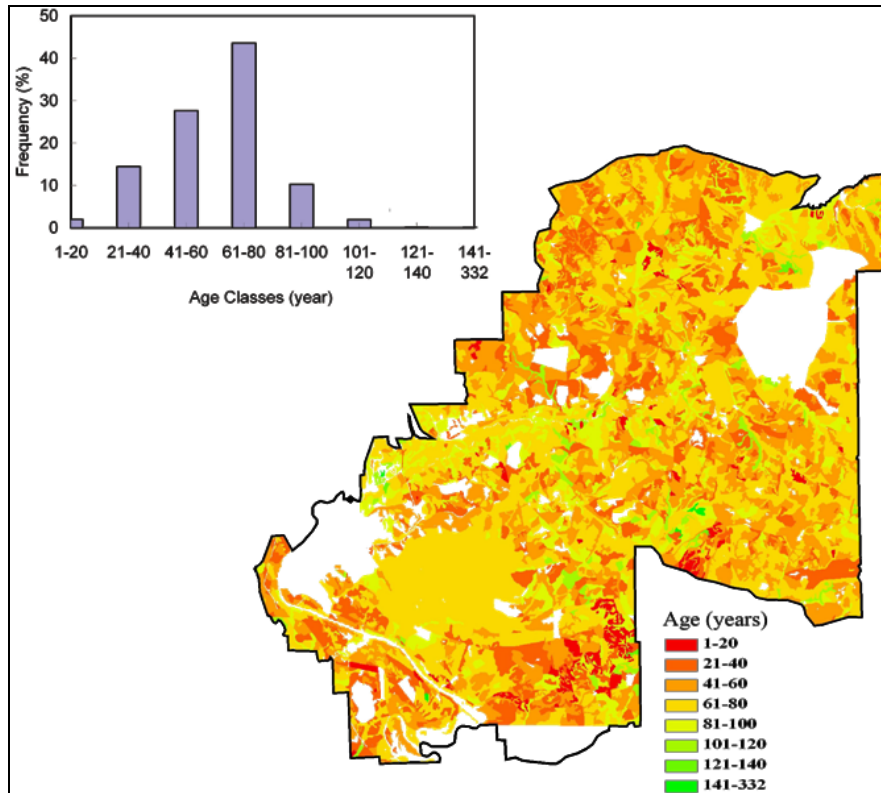


Figure 18. Fort Benning forest biomass carbon distribution according to the historical inventory data. The minimum biomass carbon were 5.3 and 175.5 Mg/ha, respectively, with an average of 51 Mg/ha.

The two databases can be used to quantify the overall changes of forest conditions at Fort Benning (Table 9). Both biomass C and basal area decreased from the historical to current inventories, probably due to selective cutting and harvesting.

Table 9. Comparison of basal area, age, and biomass carbon stocks derived from the current and historical forest inventories. (Note: the table largely reflects changes in the pine and mixed forests because the current inventory focused on these forests.)

	Historical Inventory	Current Inventory
Basal Area (m ² /ha)	15.0	11.9
Aboveground biomass (years as of 2006)	56.5	63.2
Abg biomass C (Mg/ha)	41.1	34.4
Total biomass C (Mg/ha)	58.5	50.9

However, the existing inventory databases might not be suitable for quantifying location-specific changes of age, BA, and biomass carbon (Figures 19–21). Large uncertainties still exist in the inventory databases. For example, Figure 19 (panels b and c) and Figure 21 show that BA and

biomass carbon decreased for about 70 percent of the stands from the historical to the current inventory, indicating widespread selective cutting during this period. On the other hand, carbon accumulation due to growth in some stands were obvious.

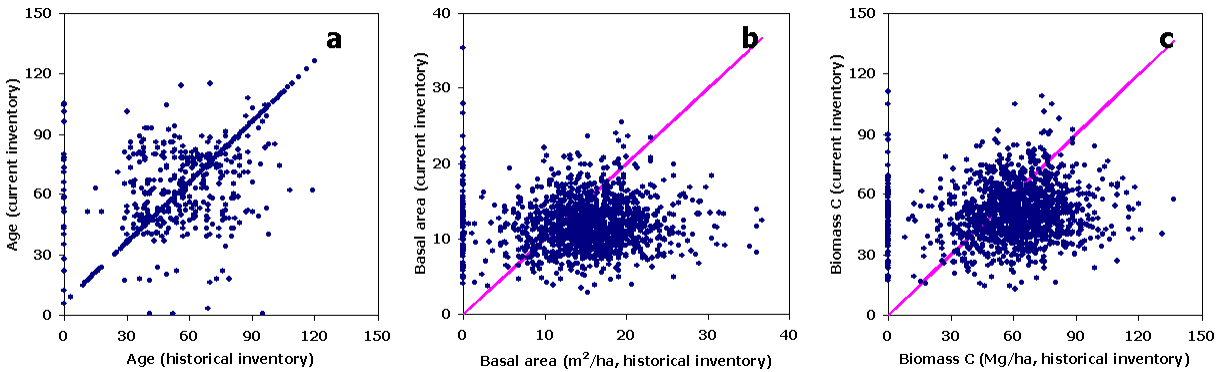


Figure 19. Comparison of forest age, basal area, and biomass carbon between the current and historical inventories. One dot represents one forest stand larger than 4 ha.

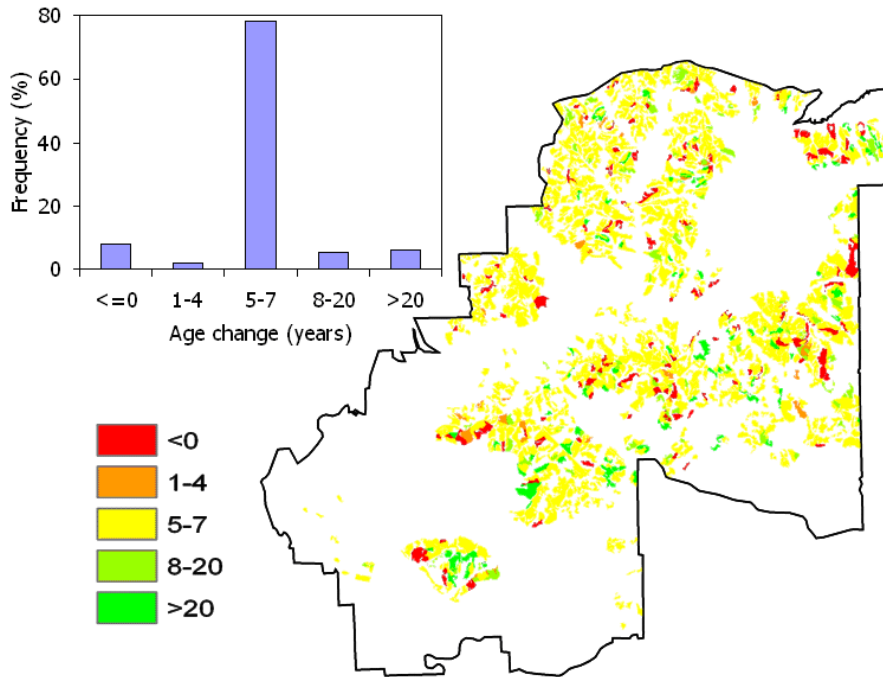


Figure 20. Age change (years) between the current and historical inventories.

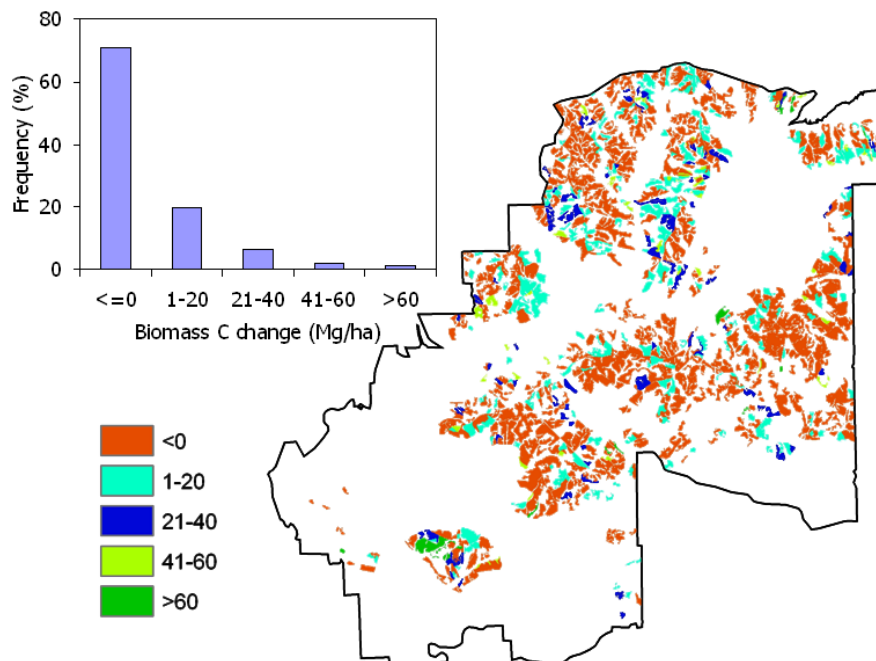


Figure 21. Total biomass carbon change (Mg/ha) between two inventory databases.

5.2 Estimating Soil Erosion and Deposition

5.2.1 USPED Erosion Estimates and Comparison with Field Observations

The soil rill erosion estimates of ten watersheds for 1999, 2001, and 2003 are shown in Figure 22. Estimated erosion varied from -0.002 to -0.180 ton/ha/year (negative sign indicates erosion) and average erosion of the ten watersheds in 1999, 2001, and 2003 was -0.06, -0.08 and -0.04 t/ha/year, respectively. In most watersheds, the highest erosion rate was in 2001, while BC1 and SB3 had their highest erosion rates in 1999.

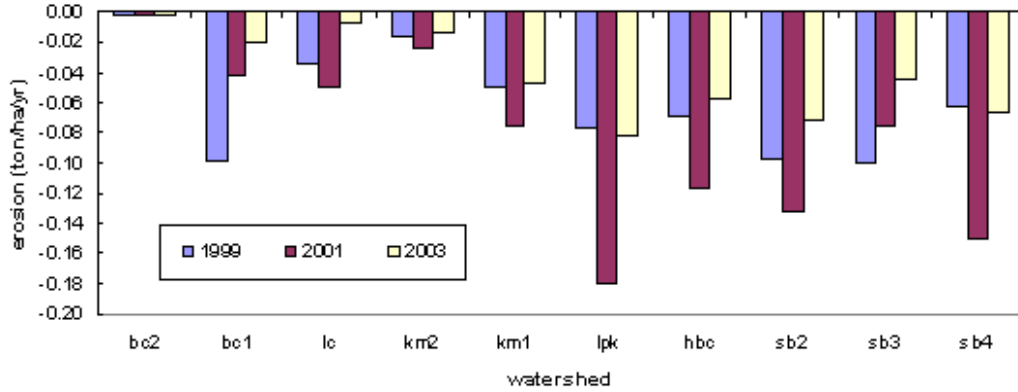


Figure 22. Estimated overall soil rill erosions in ten watersheds. Each individual watershed had its own temporal change in erosion caused by differences in land cover change.

The estimated rill erosion showed a close relationship with the total suspended sediments ($R^2 = 0.72$, see Figure 23), which was measured by Houser et al. (2006). It suggested that USPED was capable of simulating the relative magnitude of net erosion and deposition of across these catchments at Fort Benning. Once calibrated, it should be applicable to estimate the total soil erosion and deposition.

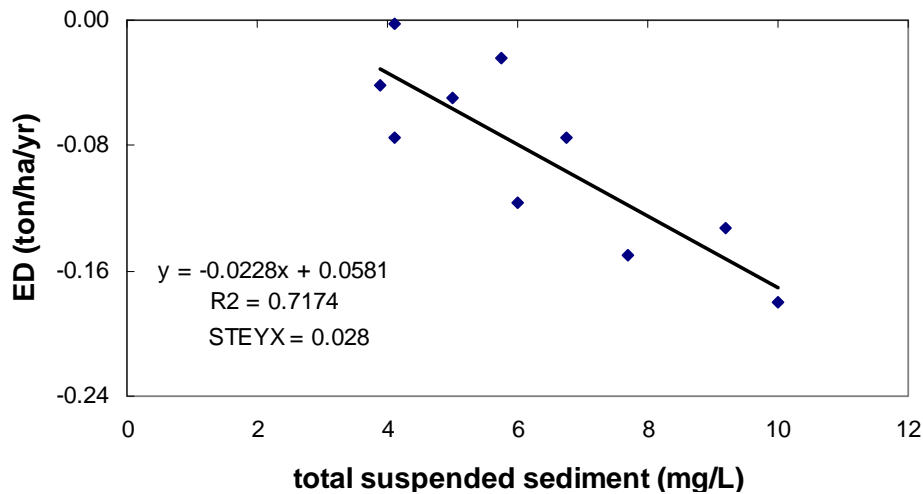


Figure 23. Relationship of estimated rill erosion using USPED with observed stream water-suspended sediment.

The capability of USPED in predicting the spatial variability of soil erosion and deposition across these catchments indicated that (1) USPED can simulate the impacts of disturbances in this region as demonstrated by the close relationships shown in Figures 23 and 24, and (2) remotely sensed imagery and related land cover maps can be used to derive estimates of the intensity of military training activities.

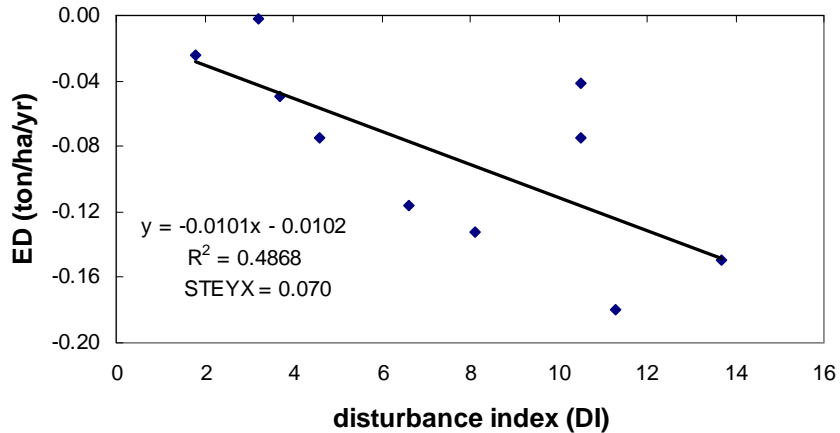


Figure 24. Relationship of estimated rill erosion using USPED with disturbance index for ten watersheds at Fort Benning, GA. On the landscape or watershed scale, military disturbances were quantified using a disturbance index (DI) as defined by Maloney et al. (2005).

5.2.2 Modeling Spatial and Temporal Changes of Soil Erosion and Deposition

USPED uses a two-dimensional divergence algorithm to calculate both erosion and deposition across the landscape. The simulated spatial distribution of soil erosion and deposition of BC1 and BC2 watersheds in 1999, 2001, and 2003 are displayed in Figure 25.

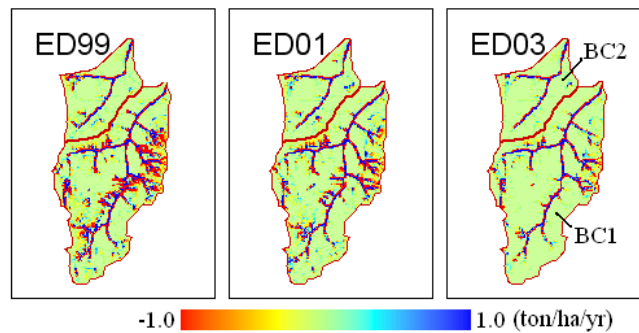


Figure 25. Spatial variation and temporal changes of soil erosion and deposition at two small watersheds at Fort Benning, GA. Display range is set to -1.0 to +1.0 ton/ha/yr to reveal spatial details of the majority of land pixels. Negative values indicate erosion.

The spatial and temporal changes in Figure 29 clearly demonstrated the impacts of disturbances and vegetation recovery on soil erosion and deposition. The high erosion sites (in red and yellow) usually were associated with grasslands and bare lands (implying heavier military training disturbance). BC1 had the highest soil erosion rate in 1999 because more bare land and grassland were detected than other two years. Vegetation recovered since 1999, which reduced

soil erosion. On the other hand, no significant change in erosion was detected in BC2. This is mainly because BC2 has been a reference catchment and no military training activities happened there from 1999 to 2003.

5.3 Simulating Impacts of Cyclic Prescribed Fire on Ecosystem C and N Cycles

5.3.1 Carbon and Nitrogen Fluxes

5.3.1.1 Net Primary Production (NPP) and Change

NPP varied greatly among different combinations of scenarios (see Figure 26a1, b1, and c1), indicating that fire management practices and how ecosystem responds to fire, specifically biologic N₂ fixation rates, have a dramatic impact on the evolution of ecosystem NPP and its end state. Maximum ecosystem NPP was realized under the combination of no fire with high level of both symbiotic and nonsymbiotic N₂ fixation rates. However, because fire is a key factor that can sustain the longleaf pine ecosystem, the above scenario is unlikely to exist in reality. With the presence of fire, the best NPP was realized under low frequency and low intensity fire with high N inputs. Lower ecosystem NPP generally occurs with higher fire frequency and intensity (higher nutrient loss) and lower N inputs. The worst case for ecosystem NPP was high fire frequency and intensity without biological N inputs (Figure 26a1). The situations of tree NPP were similar to those of ecosystem NPP (Figure 26b1), because trees are the dominant component of Fort Benning pine forest ecosystem. In contrast, the highest understory NPP was under the combination of high frequency and high intensity fire, along with high symbiotic N₂ fixation rate, and no nonsymbiotic N input. The lowest NPP for understory was without fire and with high levels of both symbiotic and nonsymbiotic N input (Figure 26c1). This was consistent with previous studies documenting that fire stimulates the growth of understory grasses (e.g., Collins et al., 1995; Pendergrass et al., 1999). The results also suggested that competition between symbiotic N₂ and nonsymbiotic N₂ fixation for understory may exist. The average conditions with different treatment levels and their differences can be seen in Figure 26a2-a5, 26b2-b5 and 26c2-3c5.

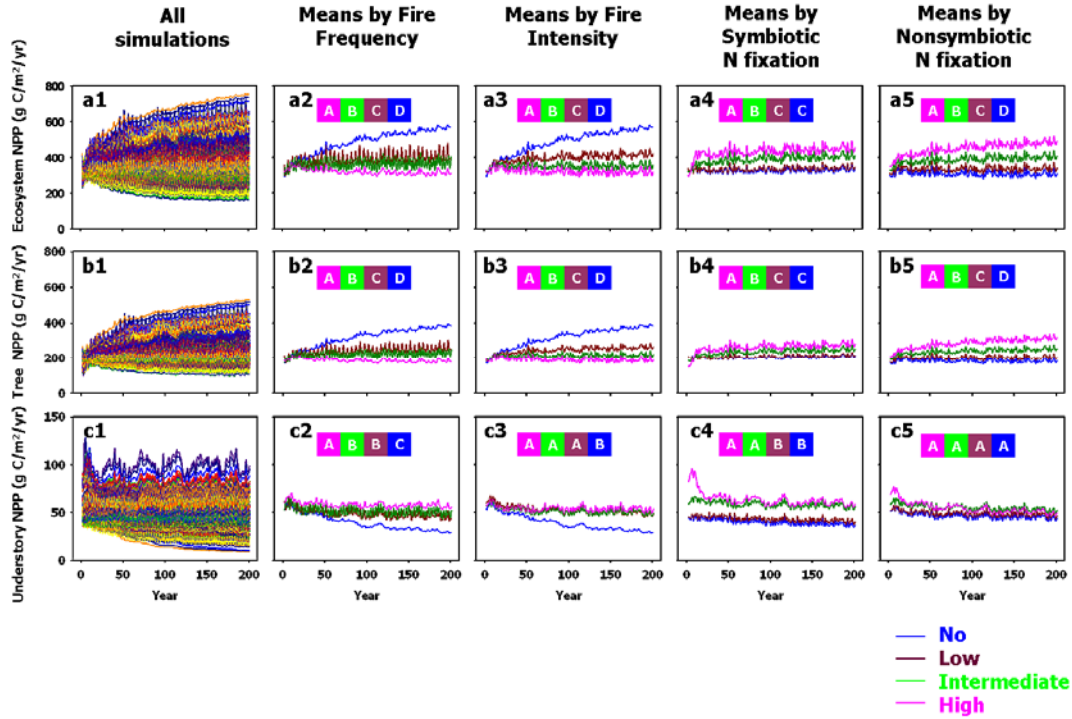


Figure 26. Impacts of fire frequency, fire intensity, symbiotic and nonsymbiotic N inputs on net primary production (NPP) of ecosystem (a), tree canopy (b), and understory (c). Values within colored squares with different capital letters denote significant difference.

Multiple regression analysis showed that both ecosystem NPP and tree NPP were correlated significantly and negatively with fire frequency and fire intensity, and related strongly and positively to symbiotic and nonsymbiotic N_2 fixation rate. Understory NPP was related significantly and positively to symbiotic N_2 fixation rate, fire frequency and fire intensity. Nonsymbiotic N_2 fixation rate was not significantly associated with understory NPP (Table 10).

Long-term NPP change trends under the impacts of different combinations of fire frequency, fire intensity, and biological N_2 fixation rates were indicated by Figure 16 with the four selected scenarios (see Table 9). Under the current fire regime (2311), both ecosystem NPP and tree NPP significantly decreased during the 200-year simulation. Under the scenarios of 1333, 2333, and 2222, both ecosystem NPP and tree NPP significantly increased over time, and the variation in NPP with 1333 was stronger and steeper than those with 2333 and 2222 (Figure 27a and 31b). Understory NPP significantly decreased during the 200-year period under the current fire regime (2311), significantly increased under the scenario of 1333, and showed no significant trend under the scenarios of 2333 and 2222 (Figure 27c). However, understory NPP with the scenario 1333 declined significantly during the first 50-year simulation. The rapidly increased trend in tree NPP with the scenario 1333 during the first 50-year period corroborated the competition between canopy and understory.

Table 10. Standardized canonical coefficient of fire frequency, fire intensity, and symbiotic and nonsymbiotic N₂ fixation rates for the prediction of NPP.

	Ecosystem NPP	Tree NPP	Understory NPP
Canonical R ²	0.94****	0.92****	0.51****
Fire frequency	-0.36****	-0.42****	0.46****
Fire intensity	-0.40****	-0.41****	0.09NS
Symbiotic N ₂ fixation rate	0.47****	0.36****	0.87****
Nonsymbiotic N ₂ fixation rate	0.62****	0.62****	-0.05NS

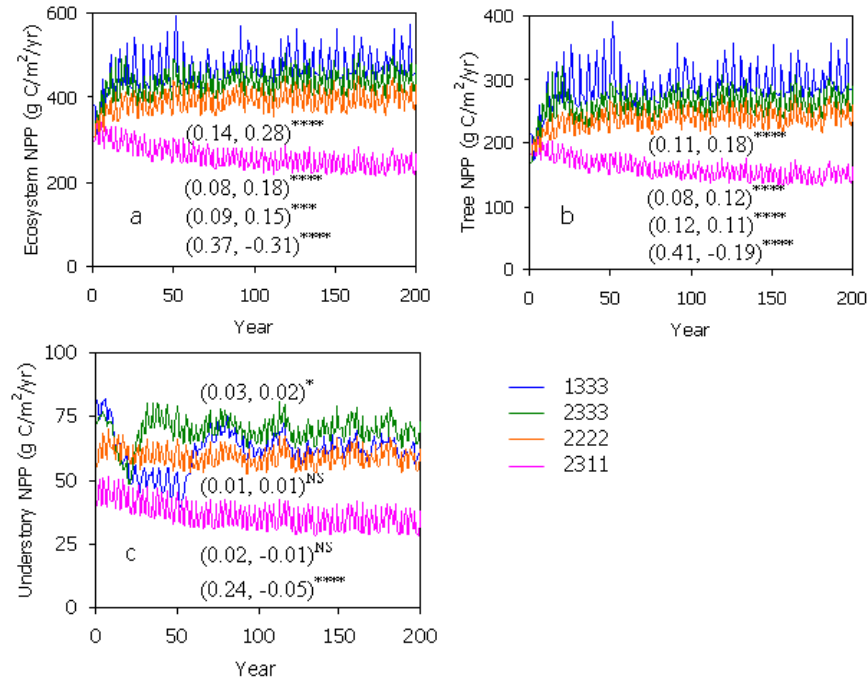


Figure 27. Long-term change trend in net primary production (NPP) of ecosystem (a), tree canopy (b), and understory (c) under four selected scenarios. The first number with scenario combination represents fire frequency, the second for fire intensity, the third for symbiotic N input, and the fourth for nonsymbiotic N input. 1, 2 and 3 represents low, intermediate and high respectively. Insert numbers denote (r², b)p, which follow the order of scenarios from top to bottom. The symbols for P value are the same as in Table 8.

5.3.1.2 Total Nitrogen Input and Net N Mineralization

Highest total N inputs occurred under the combinations of high fire frequency, high fire intensity, and high symbiotic N₂ fixation rate, irrespective of nonsymbiotic N₂ fixation rate (Figure 28a1). With the increase of fire frequency and intensity, total N input significantly increased except that low and intermediate intensity fire did not show significant difference in affecting N input into ecosystem (Figure 28a2 and a3). These suggested that a negative feedback

between herbaceous legume (N replenishment) and fire (N loss) may exist, which was in agreement with field observations showing that frequent dormant-season fire promotes the establishment, growth and reproduction of diverse native legume species (Waldrop et al., 1992; Hains et al., 1999; Hiers et al., 2000, 2003). With the increase of biological N₂ fixation rate, total N input significantly increased except that there was no significant difference in the impact of no and low symbiotic N₂ fixation on N input into ecosystem (Figure 28a4 and a5). Cyclic fire resulted in transient “pulses” of net N mineralization relative to no fire, and the maxima were realized under the combination of low fire frequency, low fire intensity, and high levels of both symbiotic and nonsymbiotic N₂ fixation rate (Figure 28b1). The “pulse” input of available N into soil following fire has been observed widely in the short-term experimental studies (e.g., Kovacic et al., 1986; Kaye and Hart, 1998). The minimum net N mineralization was with the scenario of high frequency and intensity fire without any biological N₂ fixation. Net N mineralization significantly decreased along with the increase of fire frequency and fire intensity (Figure 28b2 and b3). Compared to no and low biological N₂ fixation, intermediate and high levels of symbiotic and nonsymbiotic N₂ fixation rates significantly enhanced the net N mineralization (Figure 28b4 and b5).

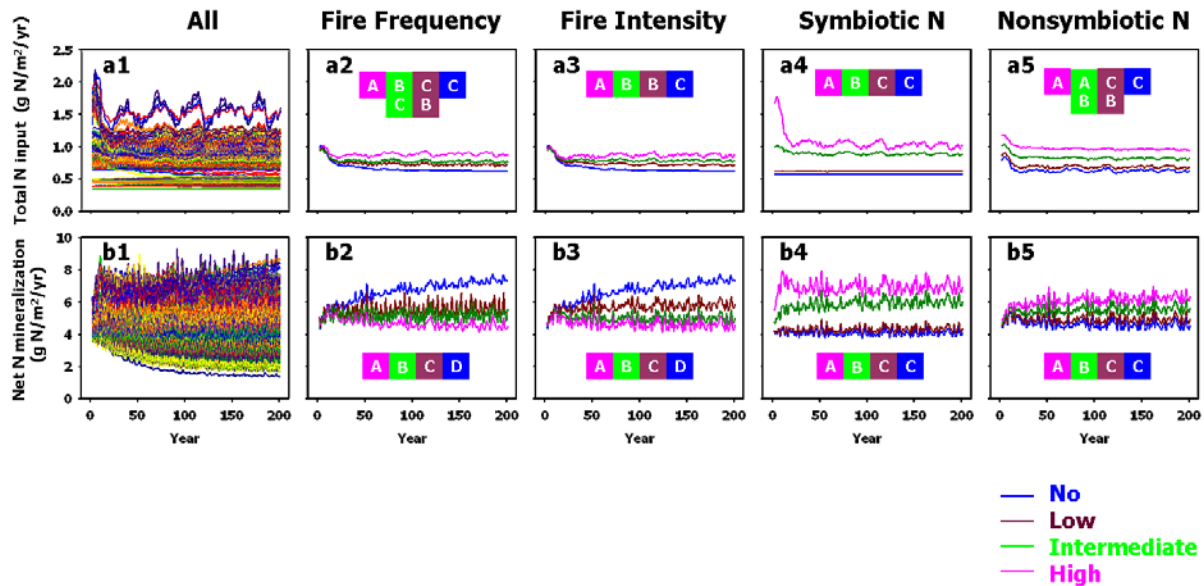


Figure 28. Impacts of fire frequency, fire intensity, symbiotic and nonsymbiotic N inputs on total N input (a) and net N mineralization (b). Total N input includes symbiotic and nonsymbiotic N₂ fixation and atmospheric N deposition. Legends are the same as in Fig 26.

Multiple regression analysis indicated that total N input was significantly and positively related to fire frequency, fire intensity, and symbiotic and nonsymbiotic N₂ fixation rate. Net N mineralization was correlated significantly and negatively with fire frequency and fire intensity, and significantly and positively with both symbiotic and nonsymbiotic N₂ fixation rate (Table 11). Symbiotic N₂ fixation rate was the most important factor affecting the variation in both total

N input and net N mineralization, suggesting that N₂-fixing legumes may play an important role in the N cycles of burned ecosystem by offsetting N loss from fire.

Table 11. Standardized canonical coefficients of fire frequency, fire intensity, and symbiotic and nonsymbiotic N₂ fixation rates for the prediction of total N input and net N mineralization.

	Total N input	Net N mineralization
Canonical R ²	0.80****	0.86****
Fire frequency	0.23***	-0.26****
Fire intensity	0.16****	-0.33****
Symbiotic N ₂ fixation rate	0.78****	0.78****
Nonsymbiotic N ₂ fixation rate	0.53****	0.39****

Long-term change trends of total N input and net N mineralization could be seen in Figure 29 with the four selected scenarios. Under the current fire regime (2311), total N input was the lowest, but it showed a significantly increasing trend during the 200-year simulation with very low slope. Total N input under the scenarios of 1333, 2333, and 2222 significantly declined over the 200-year period, and the strongest and the steepest change trends were with 2222 and 1333, respectively (Figure 33a). Under the current fire regime (2311), net N mineralization significantly decreased during the 200-year simulation. Under the scenarios of 1333, 2333, and 2222, net N mineralization increased over time, and its variation with 1333 was stronger and steeper than those with 2333 and 2222 (Figure 29b).

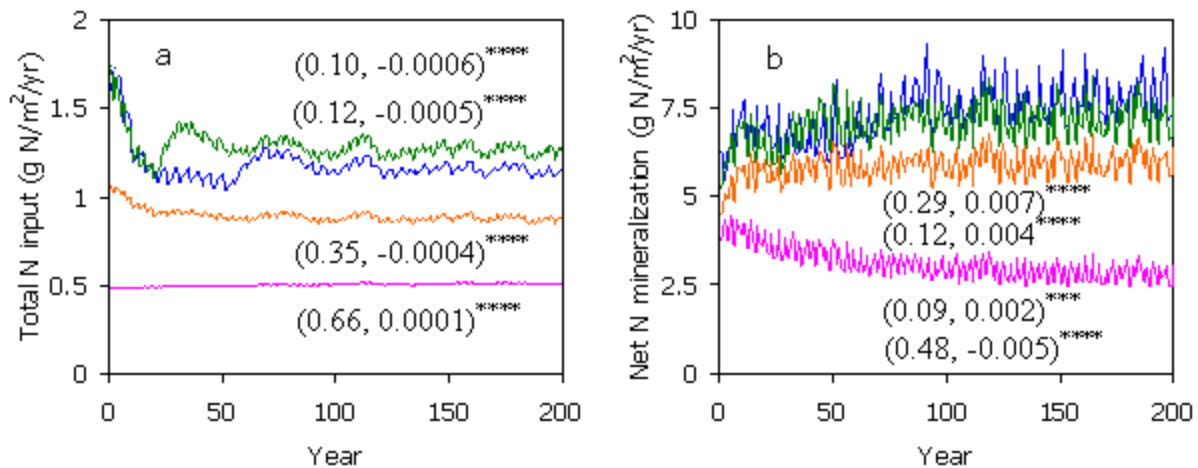


Figure 29. Long-term change trends in total N input (a) and net N mineralization (b) under the four selected scenarios. Legends are the same as in Figure 27.

5.3.2 Carbon and Nitrogen Stocks

5.3.2.1 Carbon Stocks and Changes

Ecosystem C stock (sum of biomass C, litter and soil organic carbon (SOC)) varied between 100 and 300 Mg/ha at the end of simulation (Figure 30a1). It was adversely affected by fire. With the increase of fire frequency or fire intensity, the accumulation of ecosystem C was significantly decreased. Under high frequency and high intensity of fire without biological N input, the ecosystem acted as a C source, releasing 0.16 Mg/ha/yr C into the atmosphere. Ecosystem C stock increased along with the increase of biological N₂ fixation. Although ecosystem C stocks declined under certain individual cases, on average, they did not decline for any of the treatment levels (Figure 30a2–a5).

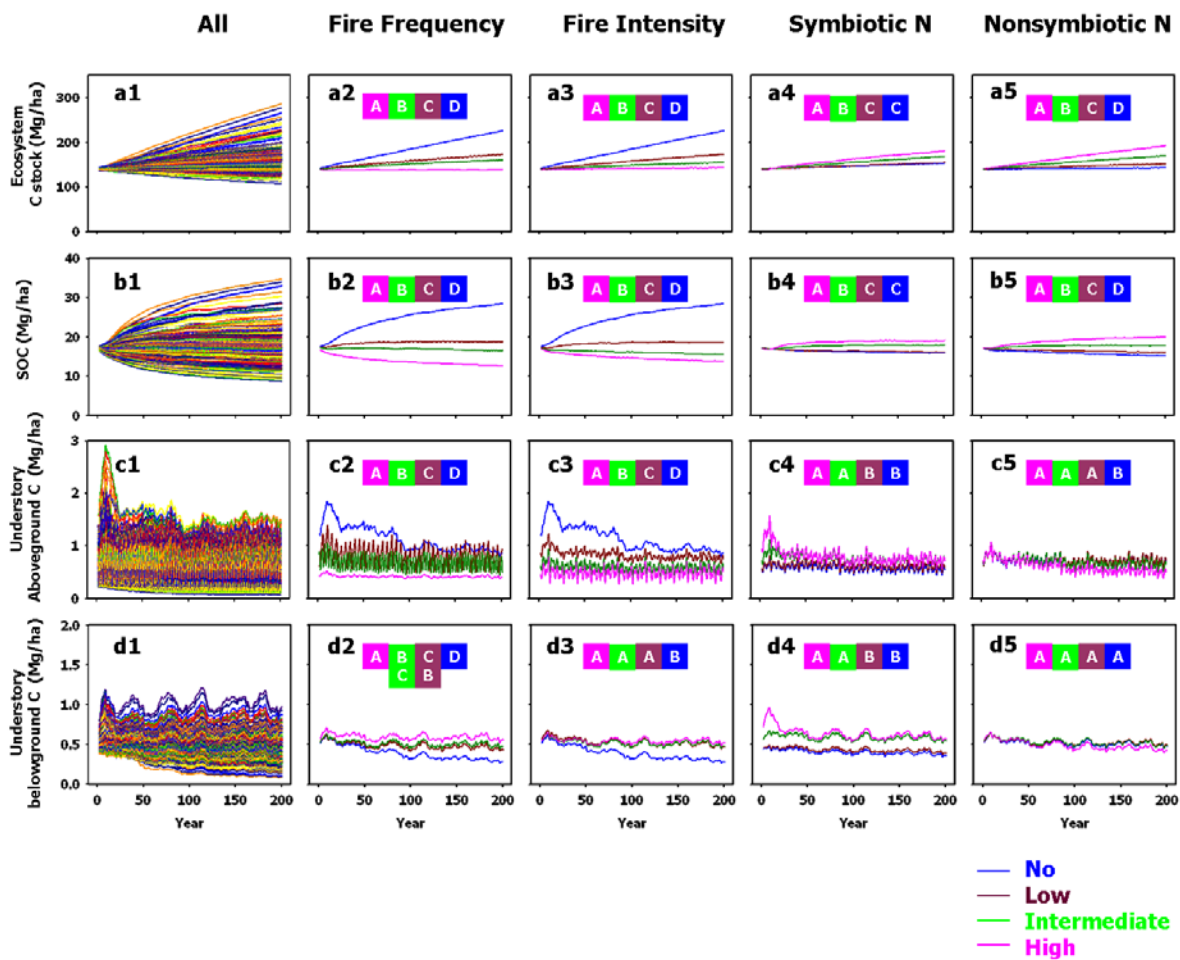


Figure 30. Impacts of fire frequency, fire intensity, symbiotic and nonsymbiotic N inputs on forest ecosystem C stock (a), soil organic carbon (SOC) (b), understory aboveground C stock (c), and understory belowground C stock (d). Legends are the same as in Figure 26.

SOC (sum of carbon in humus, particulate matters, soil microbes, and soil fungi) changed from about 17 Mg/ha at the start of simulation to 10 ~ 33 Mg/ha at the end of simulation, strongly depending on fire regime and N input. The higher SOC accumulation occurred with lower fire frequency and intensity, and higher biological N input. High frequency and intensity fire without N input caused a significant reduction in SOC, with an annual decrease rate of 0.015 Mg/ha (Figure 30b1). The average conditions with different treatment levels and their differences were shown in Figure 30b2-b5.

Understory aboveground C for all simulations were either significantly decreased or showed no significant trend during the 200-year period. Higher understory aboveground C stocks were with the combinations of lower frequency and intensity fire, higher symbiotic N₂ fixation rate and lower nonsymbiotic N₂ fixation rate (Figure 30c1-c5), suggesting that a competition may exist between symbiotic and nonsymbiotic N₂ fixation. In contrast, understory belowground C increased with the increase of fire frequency or fire intensity (Figure 30d1-d3), indicating that understory adapted to cyclic fire by storing biomass in belowground structures, consistent with earlier studies (Ojima et al., 1994; Brockway and Lewis, 1997). Two highest understory belowground C stocks were realized under the combinations of high frequency and intensity fire, high symbiotic N₂ fixation with no and low nonsymbiotic N₂ fixation (Figure 34d1). On average, intermediate and high level symbiotic N input significantly enhanced the C stock of understory relative to no and low symbiotic N input (Figure 30d4). Different levels of nonsymbiotic N₂ fixation had no significant effect on understory belowground C stock (Figure 30d5).

As indicated by Table 12, both ecosystem C stock and SOC were significantly and negatively correlated with fire frequency and fire intensity, and related significantly and positively to symbiotic and nonsymbiotic N₂ fixation rate. Fire frequency was the most important factor accounting for the variation in both ecosystem C stock and SOC. The responses of understory aboveground and belowground C stock to fire were different. Understory aboveground C stock was strongly and negatively related to fire frequency and fire intensity, significantly and negatively correlated with nonsymbiotic N₂ fixation, and significantly and positively related to symbiotic N₂ fixation. Understory belowground C stock was strongly and positively correlated with symbiotic N₂ fixation and fire frequency, had no significant relationship with fire intensity and nonsymbiotic N₂ fixation. Fire frequency and symbiotic N₂ fixation rate were the most important factors affecting understory aboveground and belowground C stock, respectively.

Table 12. Standardized canonical coefficients of fire frequency, fire intensity, and symbiotic and nonsymbiotic N₂ fixation rates for the prediction of C stocks.

		Ecosystem C stock	SOC	Understory aboveground C	Understory belowground C
Canonical R ²		0.94****	0.96****	0.74****	0.52****
Fire frequency		-0.54****	-0.63****	-0.61****	0.49****
Fire intensity		-0.42****	-0.47****	-0.51****	0.08 NS
Symbiotic fixation rate	N ²	0.31****	0.25****	0.34****	0.85****
Nonsymbiotic fixation rate	N ²	0.51****	0.32****	-0.14**	-0.07 NS

The symbols for P value are the same as in Table 12.

Figure 31 showed the long-term changes of C stocks under the four selected scenarios. Ecosystem C stock significantly decreased during the 200-year simulation under the current fire regime (2311), and significantly increased under the scenarios of 1333, 2333, and 2222. The increasing trend with 1333 was the strongest and steepest (Figure 31a). SOC declined significantly over the 200-year period under the scenarios of current fire regime (2311) and 2222, the change trend with 2311 was much stronger and steeper than that of 2222. Under the scenarios of 1333 and 2333, SOC increased over time, and its variation with 1333 was stronger and steeper than that with 2333 (Figure 31b). Under current fire regime (2311), understory aboveground C stock significantly decreased during the 200-year simulation. Under the scenarios of 1333, 2333, and 2222, understory aboveground C stock did not show significant change trends (Figure 31c). In contrast, understory belowground C stock significantly decreased over the 200-year period under the scenarios of current fire regime (2311) and 2222, the change trend with 2311 was much stronger and steeper than that of 2222. No significant change trend in SOC was observed with the scenario of 2333. SOC showed increasing trend under the scenario of 1333.

Figure 31 showed the long-term changes of C stocks under the four selected scenarios. Ecosystem C stock significantly decreased during the 200-year simulation under the current fire regime (2311), and significantly increased under the scenarios of 1333, 2333, and 2222. The increasing trend with 1333 was the strongest and steepest (Figure 31a). SOC declined significantly over the 200-year period under the scenarios of current fire regime (2311) and 2222, the change trend with 2311 was much stronger and steeper than that of 2222. Under the scenarios of 1333 and 2333, SOC increased over time, and its variation with 1333 was stronger and steeper than that with 2333 (Figure 31b). Under current fire regime (2311), understory aboveground C stock significantly decreased during the 200-year simulation. Under the scenarios of 1333, 2333, and 2222, understory aboveground C stock did not show significant change trends (Figure 31c). In contrast, understory belowground C stock significantly decreased over the 200-year period under the scenarios of current fire regime (2311) and 2222, the change trend with 2311 was much stronger and steeper than that of 2222. No significant change trend in SOC was observed with the scenario of 2333. SOC showed increasing trend under the scenario of 1333.

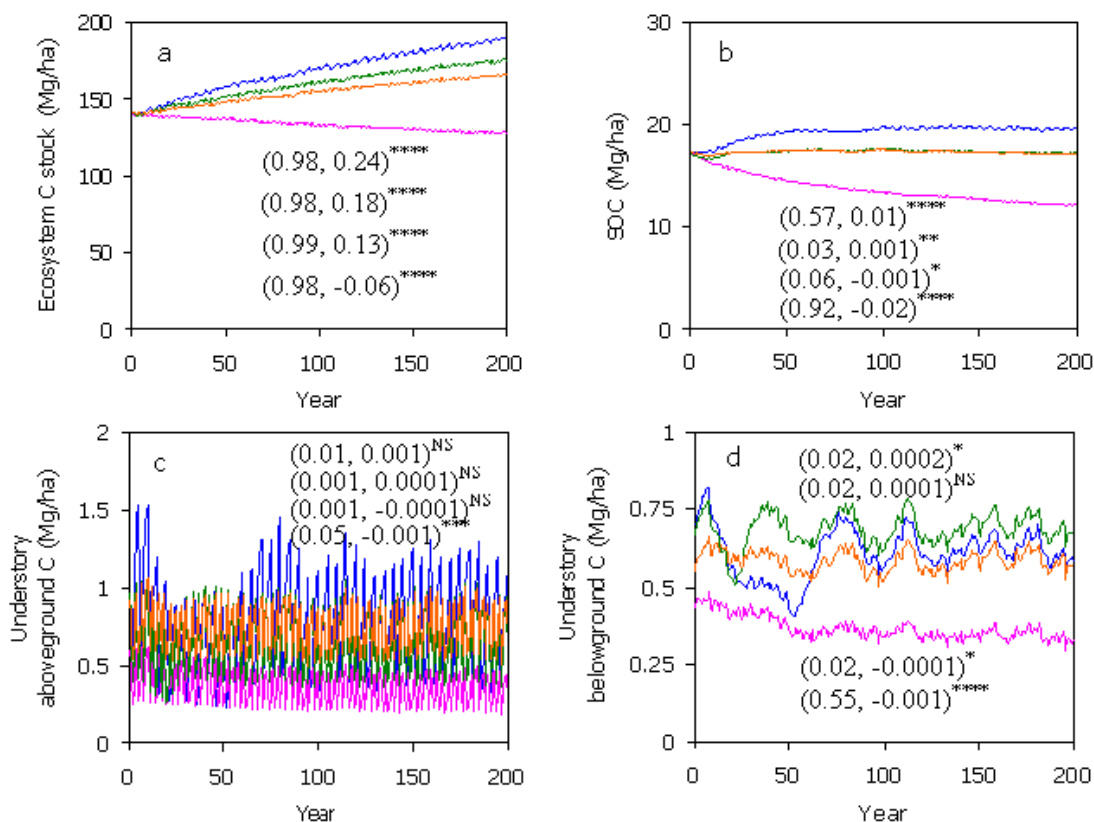


Figure 31. Long-term change trend in forest ecosystem C stock (a), soil organic carbon (SOC) (b), understory aboveground C stock (c), and understory belowground C stock (d) under the four selected scenarios. Legends are the same as in Figure 27.

5.3.2.2 Nitrogen Stocks and Changes

The N cycle in EDCM is tightly coupled with the C cycle (Figure 14). Most of the trends of N stocks were similar to those of C stocks. Total ecosystem N and soil organic nitrogen (SON) can be replenished or depleted in the future depending on fire management regimes and total N input from various sources. Frequent fire inhibited the accumulation of understory aboveground N, while promoted the accumulation of belowground N stock. Symbiotic N₂ fixation enhanced the N stock of understory, whereas nonsymbiotic N₂ fixation rate had no significant effect or even showed negative effect trend on understory N stock. This may be due to the ability of understory legumes to fix N₂. The results of N stocks and changes were shown in Figures 32 and 33, and Table 13.

The current (wet) N-deposition rate ranges 1~3 kg N per hecter per year in U.S. (e.g. Rocky Mountains). This rate varies depending on location and air quality. In general, unless acid rain becomes a negative growth factor, N-deposition will help maintain ecosystem N stock level, hence increase vegetation growth.

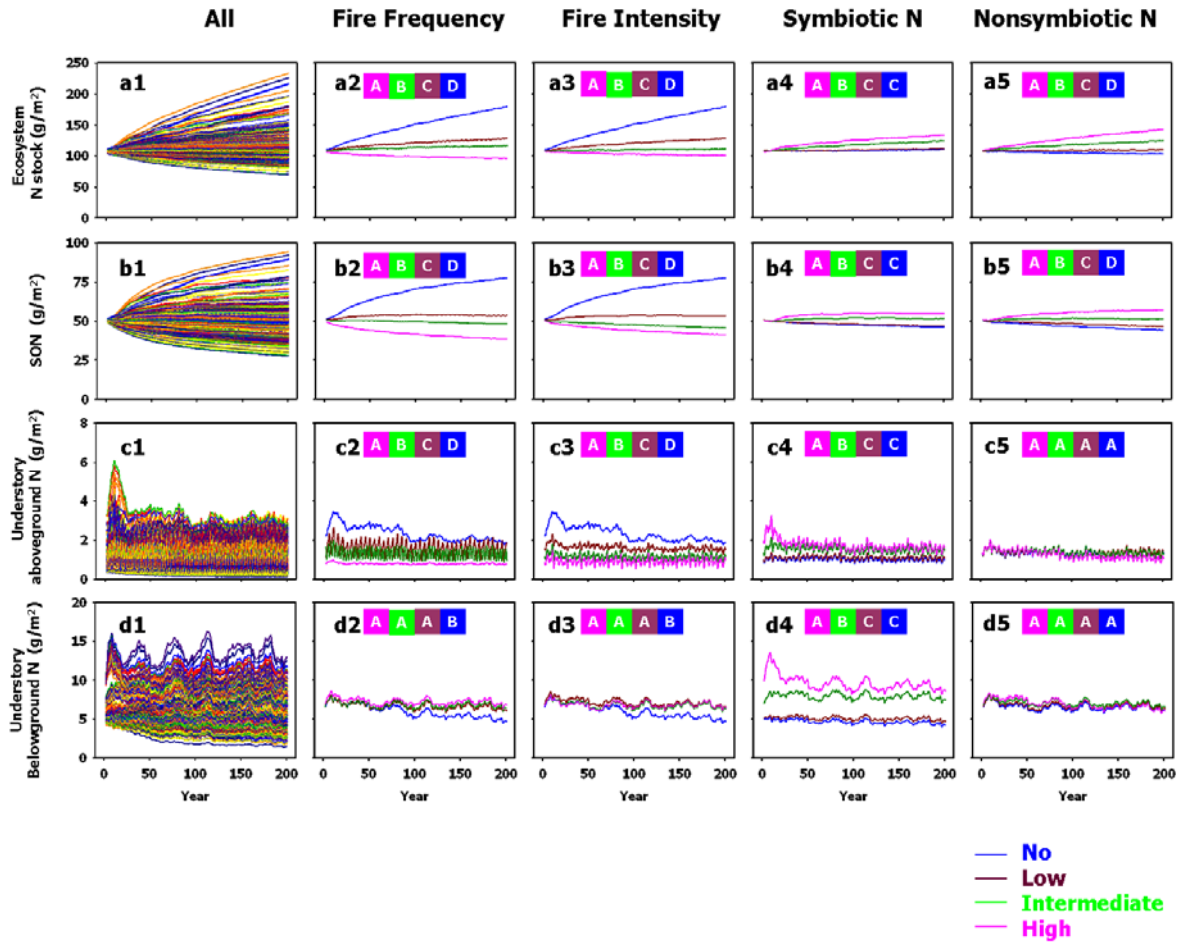


Figure 32. Impacts of fire frequency, fire intensity, symbiotic and nonsymbiotic N inputs on forest ecosystem N stock (a), soil organic nitrogen (SON) (b), understory aboveground N stock (c), and understory belowground N stock (d). Legends are the same as in Figure 26.

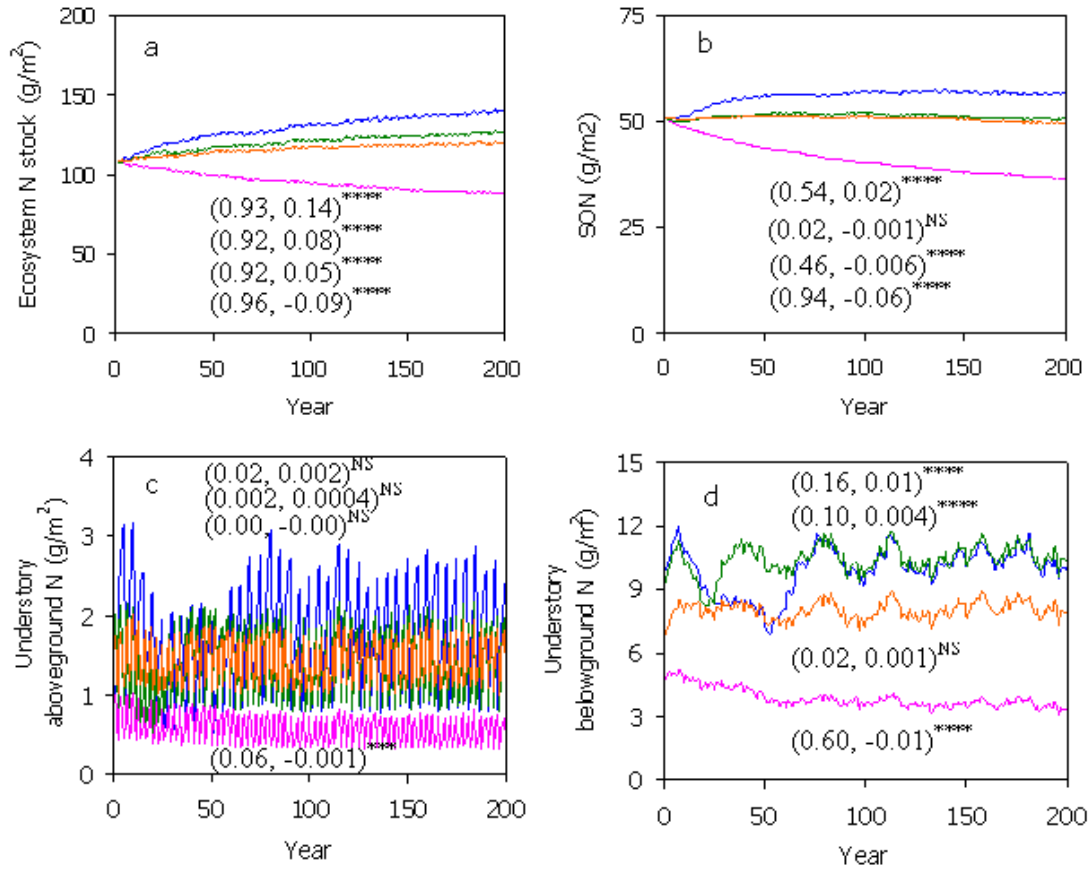


Figure 33. Long-term change trend in forest ecosystem N stock (a), soil organic nitrogen (SON) (b), understory aboveground N stock (c), and understory belowground N stock (d) under the four selected scenarios. Legends are the same as in Figure 27.

Table 13. Standardized canonical coefficient of fire frequency, fire intensity, and symbiotic and nonsymbiotic N₂ fixation rates for the prediction of N stocks.

	Ecosystem stock	N	SON	Understory aboveground N	Understory belowground N
Canonical R ²	0.94****		0.96****	0.79****	0.66****
Fire frequency	-0.55****		-0.61****	-0.56****	0.18**
Fire intensity	-0.45****		-0.47****	-0.49****	-0.03 NS
Symbiotic fixation rate	N ₂ 0.31****		0.28****	0.48****	0.98****
Nonsymbiotic fixation rate	N ₂ 0.46****		0.34****	-0.06 NS	0.09 NS

The symbols for P value are the same as in Table 12.

5.4 Differences in Carbon Sequestration between Fort Benning and Surrounding Areas

5.4.1 Comparisons of Spatiotemporal Patterns in Carbon Sequestration

The distributions of carbon sequestration for Fort Benning and surrounding areas showed a high degree of spatial heterogeneity both at present (1992–2007) and in the future (2008–2050) (Figure 34). It was apparent that the spatial occurrence or extent of carbon loss (red and pink) at Fort Benning was markedly lower than that in surrounding areas, whereas the area frequency of carbon sequestration (green and blue) was notably higher.

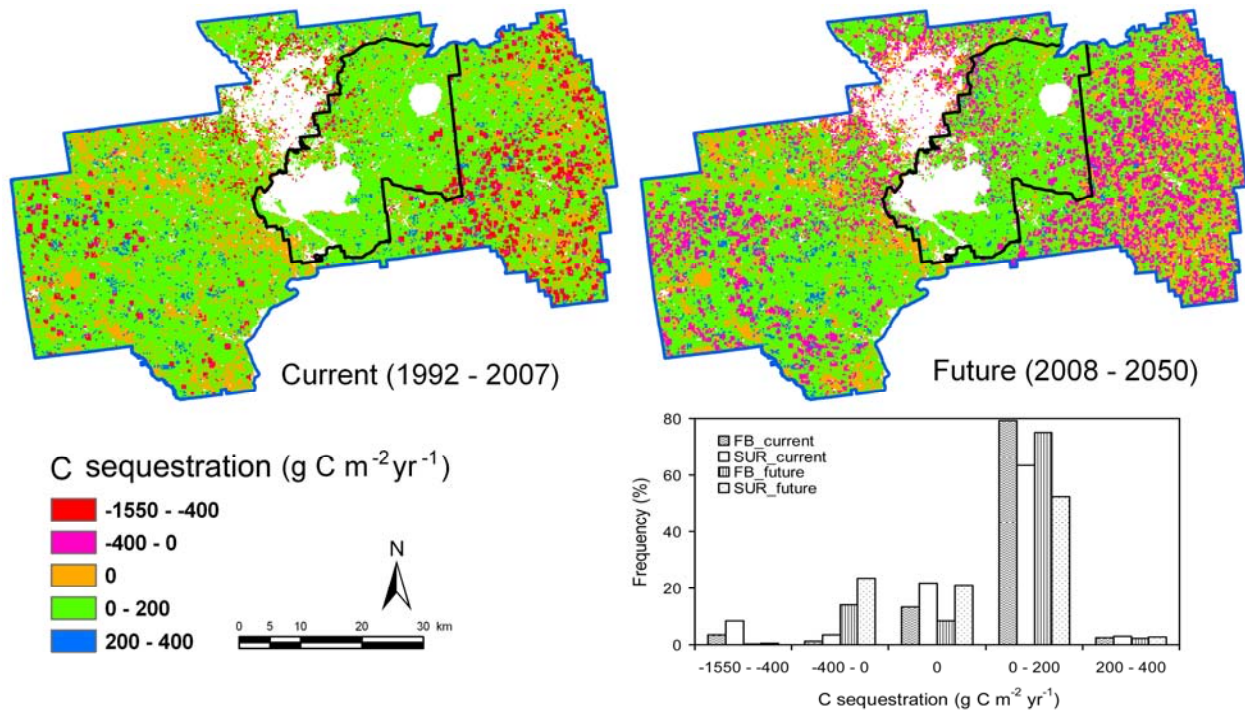


Figure 34. Spatial distributions of carbon (C) sequestration for Fort Benning (FB) and surrounding areas (SUR) during the periods 1992–2007 (current) and 2008–2050 (future). The inset graph denotes the area frequency distribution of C sequestration. A negative sequestration represents a movement of C from the landscape.

Overall, from 1992 to 2007, 4.8% of Fort Benning land area lost carbon, 13.3% was carbon neutral (orange), and 81.9% gained carbon. In contrast, the area losing carbon in surrounding areas was 11.9%, the carbon neutral area was 21.6%, and the area sequestering carbon was 66.5%. From 2008 to 2050, the areas of carbon loss, carbon neutral, and carbon sequestration were 14.3, 8.5, and 77.2% and 24, 21, and 55% for Fort Benning and surrounding areas, respectively. Meanwhile, the total carbon loss area increased from the period 1992–2007 to

2008–2050 for both Fort Benning and surrounding areas, but the magnitude of carbon release rate significantly declined, especially for surrounding areas.

The Fort Benning installation sequesters more carbon than surrounding areas at present and in the future. Average carbon sequestration rates from 1992 to 2007 and from 2008 to 2050 were 76.7 vs. 18.5 $\text{g C m}^{-2} \text{yr}^{-1}$ and 75.7 vs. 25.6 $\text{g C m}^{-2} \text{yr}^{-1}$ for Fort Benning and surrounding areas, respectively (Figure 35). Both current and future carbon sequestration demonstrated strong synchronized interannual variability for Fort Benning and surrounding areas. However, the carbon sequestration at Fort Benning was consistently higher than that in surrounding areas.

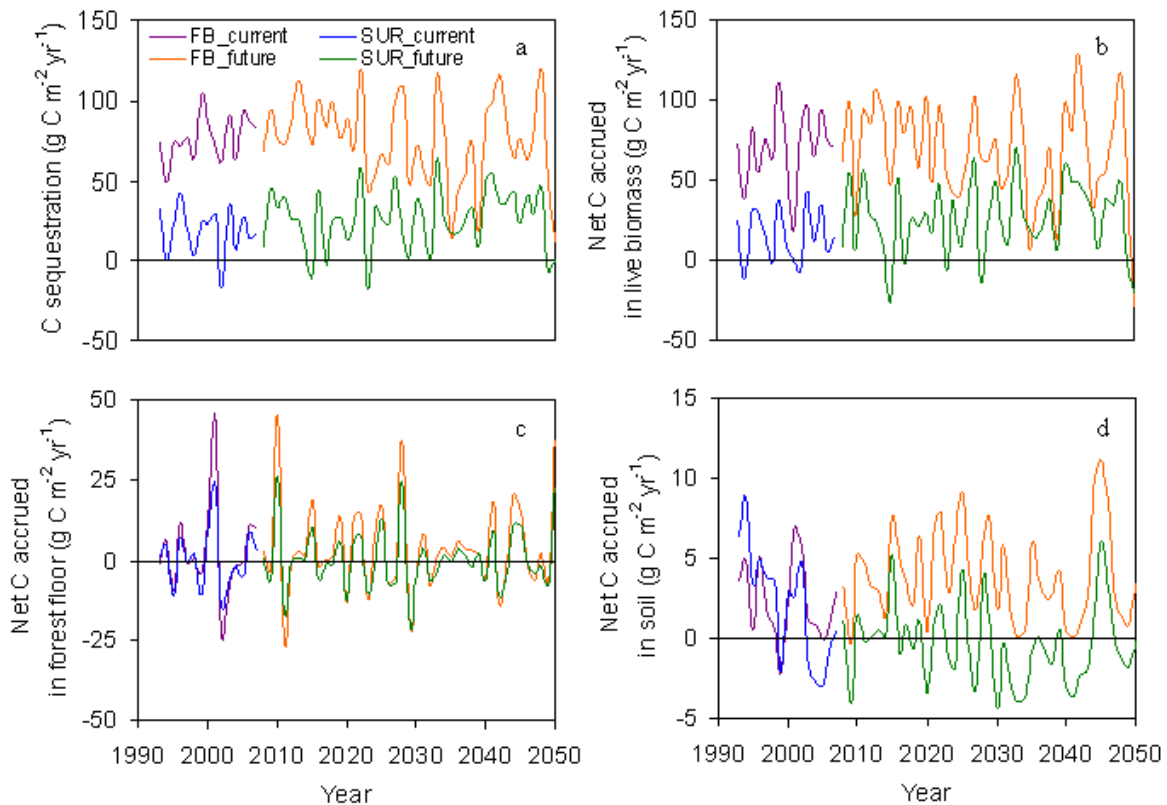


Figure 35. The contributions of net carbon (C) accrued in live biomass (b), forest floor (c), and soil (d) to ecosystem C sequestration (a).

5.4.2 Partitioning Carbon Sequestration

We partitioned the ecosystem carbon sequestration into the carbon accrued in live biomass, the forest floor, and the soil. The amount of carbon accrued in live biomass is the sum of net carbon accumulation in ecosystem live components, including leaf, fine root, fine branch, large wood, and coarse root. The amount of carbon accrued in the forest floor is the sum of net carbon accumulation in fine and coarse woody debris, and surface litter. The amount of carbon accrued

in the soil is the net accumulation of organic carbon in the top 20 cm of soil. The results demonstrated that carbon accrued in live biomass accounted for most of the carbon sequestration for Fort Benning and surrounding areas both at present and in the future (Figure 35a–d). From 1992 to 2007, the contributions of carbon accrued in live biomass, the forest floor, and the soil to ecosystem carbon sequestration for Fort Benning and surrounding areas were 92.8, 4.2, and 3.0% vs. 85.8, 2.9, and 11.3%. From 2008 to 2050, the amount of net carbon accumulated in live biomass, the forest floor, and the soil accounted for 89.7, 5.1, and 5.2% of ecosystem carbon sequestration at Fort Benning and 99.5, 1.7, and -1.2% in surrounding areas.

5.4.3 Differences between Fort Benning and Surrounding Areas

As indicated in Figure 36, annual precipitation and mean annual temperature were not significantly different between Fort Benning and surrounding areas. From 1992 to 2007, average annual precipitation and mean annual temperature were 1217 vs. 1235 mm ($P = 0.80$), and 18.0 vs. 17.6°C ($P = 0.06$) for Fort Benning and surrounding areas, respectively. From 2008 to 2050, they were 1377 vs. 1402 mm ($P = 0.55$) and 19.7 vs. 19.4°C ($P = 0.06$).

Drastic differences in land cover change were found between Fort Benning and surrounding areas. Land cover composition was relatively stable over time at Fort Benning, whereas rapid urban development at the expense of forest and cropland occurred in surrounding areas. The coverage of transitional barren (primarily caused by forest harvesting), which was negatively related to the amount of carbon accrued in live biomass, was higher in surrounding areas than at Fort Benning. From 1992 to 2050, the areal extent of transitional barren varied between 0.2 to 0.6% at the installation. In contrast, transitional barren ranged from 0.5 to 1.0% in the surrounding areas (Figure 37).

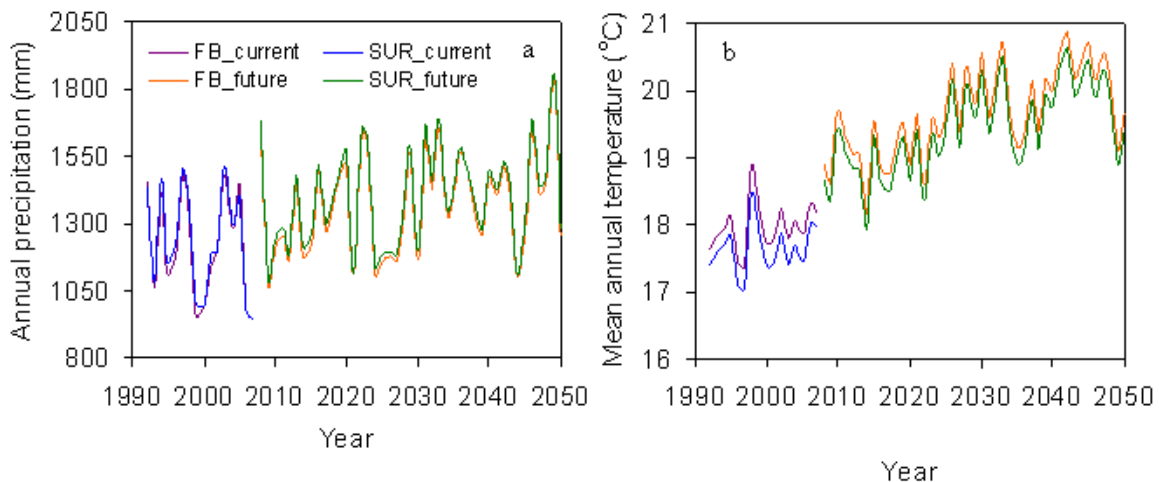


Figure 36. Temporal changes of annual precipitation (a) and mean annual temperature (b) for Fort Benning (FB) and surrounding areas (SUR) at present and in the future.

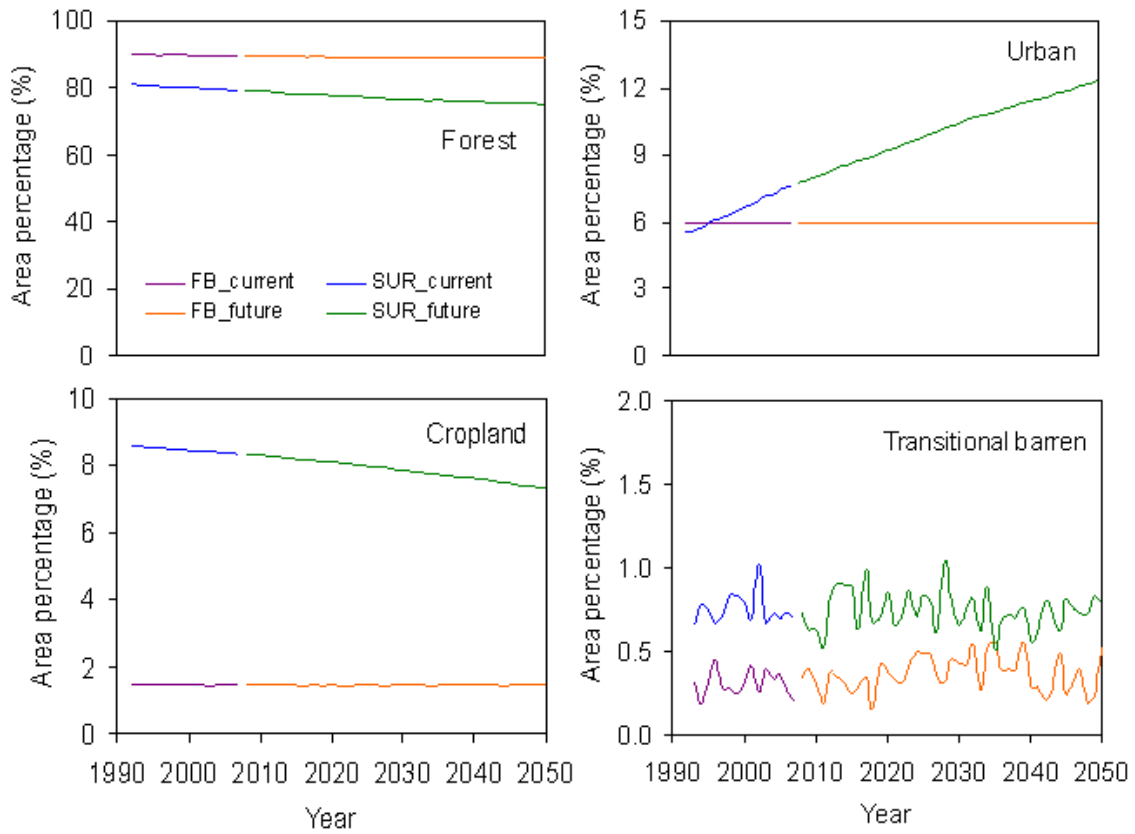


Figure 37. Current and future land cover dynamics for three major land cover types (forest, urban, and cropland) and transitional barren (caused primarily by forest harvesting) in Fort Benning and surrounding areas.

Section 6 Conclusions and Implications for Future Research/Implementation

The existing forest inventory system provides a database to generate a partial picture of the status and trends of forest resources, biomass, and carbon density. This system can be enhanced to ensure that the status and trends of forests at Fort Benning are continuously and spatially explicitly monitored. Future effort should be directed to resolving the inconsistency between historical inventory datasets and generating benchmark spatial data layers for various scientific studies and resource management. We propose: (1) establishing a number of forest field plots that can be re-measured at an interval of less than 5 years. (2) monitoring key variables of forest stand that reflect ecosystem carbon fluxes through ecosystem evolution (e.g. tree height, DBH, density, canopy cover, dead wood, ground litter stock, major management and disturbance events, and biomass removal). (3) Any ground measurements (e.g. leaf area index, canopy cover, tree phenology) that helps to calibrate remote sensing observations should also be considered.

The strong relationship between simulated net erosion and observed total suspended sediments in ten catchments indicates that USPED can be used to simulate the relative magnitudes and spatial patterns of soil erosion and deposition at Fort Benning to account for the impacts of spatial heterogeneity of biophysical conditions and military training disturbances. The simulated spatial variability of soil erosion and deposition can be useful for strategically planning military training activities spatially to minimize the impacts of disturbances. Remotely sensed data can be valuable in monitoring the spatial and temporal dynamics of erosion and deposition on landscape in response to disturbances. Several aspects need improvements: (1) link soil moisture budget with curve number; (2) obtain additional C-factors for unpaved roads and other types of mechanistically disturbed land; and (3) build an automatic, dynamic parallel computing mechanism. This is because the process of GEMS-EDCM-USPED modeling is very inefficient in current model structure. We plan to continue this study by building GEMS-EDCM into a completely parallel system in the near future. Then more management case studies, especially erosion related, will be better implemented.

Model simulations indicated that cyclic prescribed fire had significant impacts on long-term equilibrium status of C and N fluxes and stocks, ecosystem productivity, and ecosystem sustainability at Fort Benning. From simulation results and statistical analyses, the consequence of prescribed burning is generally a net removal of ecosystem nutrient and potentially a negative effect on ecosystem productivity because of loss of nutrients. Ecosystem NPP would be the lowest with high fire frequency and intensity without biological N inputs. Without fire and with high levels of both symbiotic and nonsymbiotic N input, understory NPP would be the lowest. Use of high frequency and high intensity fires will likely bring a negative effect on ecosystem productivity. Low and medium fire frequency and intensity are generally acceptable as management options because of no major productivity degradation. However, the changes in N cycle due to prescribed fire could be more complicated than current model can represent. The ecosystem nutrient inputs from N deposition, N fixation, and fertilization were not fully studied in this project. We didn't have in-depth analyses on nitrogen fixation yet. Nitrogen fixation is one of the direct drivers for ecosystem productivity. Given a nitrogen fixation level, its effect on

productivity is dependent on vegetation type, biomass stock level, soil N pool, and possibly climate. These uncertainty areas need to be addressed before more specific quantitative answers can be provided to managers about unsustainable levels of fire frequency and intensity. The model simulations leave other questions to answer: 1) How fire affects the long-term ecosystem nutrient dynamics and how the ecosystem responds to fire depend mainly on both fire regime and N input from various sources, and 2) How to balance N loss from fire and N replenishment from biological N₂ fixation, N deposition or fertilizer applications is the key to manage and restore longleaf pine ecosystem. These results emphasize a need to more fully understand the interactions between different fire regimes (e.g., frequency, intensity and season) and abundance, diversity of legume species and associated N₂ fixation. Furthermore, additional studies on biological feedbacks of ecosystem following fire, such as plant nutrient use efficiency, and belowground production and turnover are critically needed to understand the mechanisms of fire effects and to effectively manage fire maintained ecosystems.

Using GEMS, which is capable of dynamically assimilating land use change information into the simulation process over large spatial extents, combined with consistent, high-quality, and spatially explicit LUCC databases, this study simulated and compared spatiotemporal patterns in ecosystem carbon sequestration between the U.S. Army's Fort Benning installation and surrounding areas from 1992 to 2050. The results indicate that the military installation sequestered more carbon than surrounding areas at present and in the future. Differences in land use activities were the primary cause behind the difference in carbon sequestration magnitudes.

Military installations, which cover approximately 12.3 Mha of land throughout the United States (AFA, 1992), might play a significant role in sequestering and conserving atmospheric carbon because the military can adopt proactive management approaches, and some anthropogenic disturbances (e.g., urbanization, forest harvesting, and agriculture) can be minimal or absent on military training lands.

References

- Achard, F., Eva, H.D., Mayaux, P., Stibig, H.J., Belward, A., 2004. Improved estimates of net carbon emissions from land cover change in the tropics for the 1990s, *Global Biogeochemical Cycles*, 18, GB2008, doi:10.1029/2003GB002142.
- Alimohammadi, A., Sheshangosht, S., Soltani, M.J., 2006. Evaluation of relations between DEM-Based USPED Model Output and Satellite-based spectral indices. Conference Proceedings of Map India 2006. <http://www.gisdevelopment.net/proceedings/mapindia/2006/index.htm>
- American Forestry Association (AFA), 1992. Enhancing management of forests and vegetation on Department of Defense lands: Opportunities, benefits, and feasibility, 230-R-005, US EPA Office of Planning and Evaluation, Washington, DC.
- Baskaran, L.M., Dale, V.H., Efrogmson, R.A., Birkhead, W., 2006. Habitat modeling within a regional context: an example using gopher tortoise, *American Midland Naturalist*, 155, 335–351.
- Blanco, A.C., Nadaoka, K., 2006. A comparative assessment and estimation of potential soil erosion rates and patterns in Laguna Lake watershed using three models: Towards development of an erosion index system for integrated watershed-lake management. Symposium on Infrastructure Development and the Environment, 7–8 December 2006, SEAMEO-INNOTECH, University of the Philippines, Diliman, Quezon City, PHILIPPINES
- Bormann, B.T., Bormann, F.H., Bowden, W.B., Pierce, R.S., Hamburg, S.P., Wang, D., Snyder, M.C., Li, C.Y., Ingersoll, R.C., 1993. Rapid N₂ fixation in pines, alder, and locust - evidence from the sandbox ecosystem study. *Ecology* 74, 583–598.
- Brockway, D.G., Lewis, C.E., 1997. Long-term effects of dormant-season prescribed fire on plant community diversity, structure and productivity in a longleaf pine wiregrass ecosystem. *Forest Ecology and Management*, 96, 167–183.
- Brown, S., Schroeder, P., Birdsey, R., 1997. Aboveground biomass distribution of US eastern hardwood forests and the use of large trees as an indicator of forest development. *Forest Ecology and Management*, 96, 37–47.
- Cairns, M.A., Brown, S., Helmer, E.H., Baumgardner, G.A., 1997. Root biomass allocation in the world's upland forests. *Oecologia*, 111, 1–11.
- Chapin, F.S., Woodwell, G.M., Randerson, J.T. et al., 2006. Reconciling carbon-cycle concepts, terminology, and methods, *Ecosystems*, 9, 1041–1050.

- Chen, W., Chen, J., Cihlar, J., 2000. An integrated terrestrial ecosystem carbon-budget model based on changes in disturbance, climate, and atmospheric chemistry, *Ecological Modelling*, 135, 55–79.
- Christensen, N.L., 1987. The biogeochemical consequences of fire and their effects on the vegetation of the coastal plain of the southeastern United States. In: Trabaud, L. (Ed.), *The Role of Fires in Ecological Systems*. SPB Academic Publishers, The Hague, Netherlands, pp. 1–21.
- Collins, S.L., Glenn, S.M., Gibson, D.J., 1995. Experimental-analysis of intermediate disturbance and initial floristic composition - decoupling cause and effect. *Ecology*, 76, 486–492.
- DeBusk, W.F., Skulnick, B.L., Prenger, J.P., Reddy, K.R., 2005. Response of soil organic carbon dynamics to disturbance from military training. *Journal of Soil and Water Conservation*, 60, 163–171.
- Distefano, J.F., Gholz, H.L., 1989. Nonsymbiotic biological dinitrogen fixation (acetylene-reduction) in an age sequence of slash pine plantations in North Florida. *Forest Science*, 35, 863–869.
- Doe III, W.W. et al., 1999. *The Soil Erosion Model Guide for Military Land Mangers: Analysis of Erosion Models for Natural and Cultural Resources Applications*. Technical report for the Tri-Service CADD/GIS Technology Center, Natural and Cultural Resources Field Working Group. (Technical Report ITL 99-XX).
- Eisele, K.A., Schimel, D.S., Kapustka, L.A., Parton, W.J., 1989. Effects of available p-ratio and N:P ratio on nonsymbiotic dinitrogen fixation in tallgrass prairie soils. *Oecologia*, 79, 471–474.
- Fang, J.Y., Chen, A.P., Peng, C.H., Zhao, S.Q., Ci, L., 2001. Changes in forest biomass carbon storage in China between 1949 and 1998. *Science*, 292, 2320–2322.
- Foley, J. A., Prentice, I.C., Ramunkutty, N., Levis, S., Pollard, D., Sitch, S., Haxeltine, A., 1996. An integrated biosphere model of land surface process, terrestrial carbon balance and vegetation dynamics. *Global Biogeochem. Cycles* 10, 603–628.
- Garten, C.T., 2006. Predicted effects of prescribed burning and harvesting on forest recovery and sustainability in Southwest Georgia, USA. *Journal of Environmental Management*, 81, 323–332.
- Garten, C.T., Ashwood, T.L., 2004a. Land Cover Differences in Soil Carbon and Nitrogen at Fort Benning Georgia (ORNL/TM- 2004/14). Oak Ridge National Laboratory, Oak Ridge, TN, 37830.

- Garten, C.T., Ashwood, T.L., 2004b. Modeling soil quality thresholds to ecosystem recovery at Fort Benning, GA, USA. *Ecological Engineering*, 23, 351–369.
- Gilliam, F.S., Platt, W.J., 1999. Effects of long-term fire exclusion on tree species composition and stand structure in an old-growth *Pinus palustris* (Longleaf pine) forest. *Plant Ecology*, 140, 15–26.
- Glitzenstein, J.S., Streng, D.R., Wade, D.D., 2003. Fire frequency effects on longleaf pine (*Pinus palustris*, P. Miller) vegetation in South Carolina and Northeast Florida, USA. *Natural Areas Journal*, 23, 22–37.
- Hahn, C.D., Graves, M.R., Price, D.L., 2001. S-Tracker Survey of Sites for Long-Term Erosion/Deposition Monitoring. SERDP report: ERDC/EL TR-01-18.
<https://www.denix.osd.mil/denix/Public/Library/SEMP/Monitoring/tr-01-18.html>
- Hains, M.J., Mitchell, R.J., Palik, B.J., Boring, L.R., Gjerstad, D.H., 1999. Distribution of native legumes (Leguminosae) in frequently burned longleaf pine (Pinaceae)-wiregrass (Poaceae) ecosystems. *American Journal of Botany*, 86, 1606–1614.
- Hendricks, J.J., Boring, L.R., 1999. N₂-fixation by native herbaceous legumes in burned pine ecosystems of the Southeastern United States. *Forest Ecology and Management*, 113, 167–177.
- Hiers, J.K., Mitchell, R.J., Boring, L.R., Hendricks, J.J., Wyatt, R., 2003. Legumes native to longleaf pine savannas exhibit capacity for high N₂-fixation rates and negligible impacts due to timing of fire. *New Phytologist*, 157, 327–338.
- Hiers, J.K., Wyatt, R., Mitchell, R.J., 2000. The effects of fire regime on legume reproduction in longleaf pine savannas: is a season selective? *Oecologia*, 125, 521–530.
- Houghton, R.A., 2003. Revised estimates of the annual net flux of carbon to the atmosphere from changes in land use and land management 1850–2000, *Tellus B*, 55, 378–390.
- Houghton, R.A., and Goodale, C.L., 2004. Effects of land-use change on the carbon balance of terrestrial ecosystems, in *Ecosystems and Land Use Change*, edited by DeFries, R.S., Asner, G.P., Houghton, R.A. pp. 85–98, American Geophysical Union, Washington, DC.
- Houghton, R.A., Hackler, J.L., Lawrence, K.T., 1999. The U.S. carbon budget: contributions from land-use change, *Science*, 285, 574–578.
- Houser, J.N., Mulholland, P.J., Maloney, K.O., 2006. Upland Disturbance Affects Headwater Stream Nutrients and Suspended Sediments during Baseflow and Stormflow. *J. Environ Qual.*, 35, 352–365.

- Kauppi, P.E., Ausubel, J.H., Fang, J.Y., Mather, A.S., Sedjo, R.A., Waggoner, P.E., 2006. Returning forests analyzed with the forest identity, *Proceedings of the National Academy of Sciences of the United States of America*, 103, 17574–17579.
- Kaye, J.P., Hart, S.C., 1998. Ecological restoration alters nitrogen transformations in a ponderosa pine bunchgrass ecosystem. *Ecological Applications*, 8, 1052–1060.
- Kovacic, D.A., Swift, D.M., Ellis, J.E., Hakonson, T.E., 1986. Immediate effects of prescribed burning on mineral soil-nitrogen in ponderosa pine of New-Mexico. *Soil Science*, 141, 71–76.
- Kwilosz, J.R., Knutson, R.L., 1999. Prescribed fire management of Karner blue butterfly habitat at Indiana Dunes National Lakeshore. *Natural Areas Journal*, 19, 98–108
- Landsberg, J.J., Waring, R.H., 1997. A generalised model of forest productivity using simplified concepts of radiation- use efficiency, carbon balance and partitioning. *Forest Ecology and Management*, 95, 209–228.
- Lajeunesse, S.D., Dilustro, J.J., Sharitz, R.R., Collins, B.S., 2006. Ground layer carbon and nitrogen cycling and legume nitrogen inputs following fire in mixed pine forests. *American Journal of Botany*, 93, 84–93.
- Liu, S.G., Bliss, N., Sundquist, E., Huntington, T.G., 2003. Modeling carbon dynamics in vegetation and soil under the impact of soil erosion and deposition, *Global Biogeochemical Cycles*, 17, 1074, doi:10.1029/2002GB002010.
- Liu, S.G., Quantifying the spatial details of carbon sequestration potential and performance, in *Science and Technology of Carbon Sequestration*, edited by B. McPherson and E. Sundquist, American Geophysical Union, in press.
- Liu, S.G., Loveland, T.R., Kurtz, R.M., 2004a. Contemporary carbon dynamics in terrestrial ecosystems in the Southeastern plains of the United States, *Environmental Management*, 33, S442–S456.
- Liu, S., Kaire, M., Wood, E., Diallo, O., Tieszen, L.L., 2004b. Impacts of land use and climate change on carbon dynamics in south-central Senegal. *Journal of Arid Environments*, 59, 583–604.
- Loveland, T.R., Sohl, T.L., Stehman, S.V., Gallant, A.L., Sayler, K.L., Napton, D.E., 2002. A strategy for estimating the rates of recent United States land-cover changes, *Photogrammetric Engineering and Remote Sensing*, 68, 1091–1099.
- Madden, E.M., Hansen, A.J., Murphy, R.K., 1999. Influence of prescribed fire history on habitat and abundance of passerine birds in northern mixed-grass prairie. *Canadian Field-Naturalist*, 113, 627–640.

- Maloney, K.O., Mulholland, P.J. and Feminella, J.W. 2005. Influence of catchment-scale military land use on stream physical and organic matter variables in small Southeastern Plains catchments (USA). *Environ. Manage.*, 35, 677–691.
- McGuire, A.D., Esser, G., Foler, J., Heimann, M., Joos, F., Kaplan, J., Kicklighter, D. W., Melillo, R. A., Meier, J. M., Moore, B. III., Prentice, I. C., Ramankutty, N., Reichenau, T., Schloss, A., Tian, H., William, L. J., Wittenberg, U., Sitch, S., Clein, J. S., and Dargaville, R., 2001. Carbon balance of the terrestrial biosphere in the twentieth century: Analyses of CO₂, climate and land use effects with four process-based ecosystem models, *Global Biogeochemical Cycles*, 15, 183–206.
- McGuire, A.D., Xiao, X., Helfrich, J., Moore, B. III, Vorosmarty, C. J., Schloss, A. L., Melillo, J. M., Kicklighter, D. W., and Pan, Y., 1997. Equilibrium responses of global net primary production and carbon storage to doubled atmospheric carbon dioxide: sensitivity to changes in vegetation nitrogen concentration, *Global Biogeochemical Cycles*, 11, 173–189.
- Melillo, J. M. et al., 1995. Vegetation/ecosystem modeling and analysis project: comparing biogeography and biogeochemistry models in a continental-scale study of terrestrial ecosystem responses to climate change and CO₂ doubling, *Global Biogeochemical Cycles*, 9, 407–437.
- Metherell, A.K., Harding, L.A., Cole, C.V., Parton, W.J., 1993. CENTURY Soil Organic Matter Model Environment: Technical Documentation, Agroecosystem Version 4.0, Tech. Rep. 4, Great Plains Syst. Res. Unit, Fort Collins, Colo.
- Mitasova, H., Hofierka, J., Zlocha, M., Iverson, L.R., 1996. Modeling topographic potential for erosion and deposition using GIS. *International Journal of GIS* v. 10, no. 5, p.629–641.
- Mitas, L., Mitasova, H., 1998. Distributed soil erosion simulation for effective erosion prevention, *Water Resources Research*, Vol. 34, 505–516
- Moore, I.D., G.J. Burch., 1986. Physical basis of the length-slope factor in the Universal Soil Loss Equation. *Soil Science Society of America Journal*, 50, 1294–1298.
- Neary, D.G., Klopatek, C.C., DeBano, L.F., Ffolliott, P.F., 1999. Fire effects on belowground sustainability: a review and synthesis. *Forest Ecology and Management*, 122, 51–71.
- Newland, J.A., DeLuca, T.H., 2000. Influence of fire on native nitrogen-fixing plants and soil nitrogen status in ponderosa pine - Douglas-fir forests in western Montana. *Canadian Journal of Forest Research*, 30, 274–282.
- Noss, R.F., 1989. Longleaf pine and wiregrass: keystone components of an endangered ecosystem. *Natural Areas Journal*, 9, 211–213.

- Ojima, D.S., Schimel, D.S., Parton, W.J., Owensby, C.E., 1994. Long-term and short-term effects of fire on nitrogen cycling in tallgrass prairie. *Biogeochemistry*, 24, 67–84.
- Pan, Y., Pitelka, L.F., Hibbard, K. et al., 1998. Modeled responses of terrestrial ecosystems to elevated atmospheric CO₂: A comparison of simulations by the biogeochemistry models of the Vegetation/Ecosystem Modeling and Analysis Project (VEMAP), *Oecologia*, 114, 389–404.
- Parton, W.J., Schimel, D.S., Cole, C.V., and Ojima, D.S., 1987. Analysis of factors controlling soil organic matter levels in Great Plains grasslands, *Soil Science Society of America Journal*, 51, 1173–1179.
- Parton, W.J., Scurlock, J.M.O., Ojima, D.S., Gilmanov, T.G., Scholes, R.J., Schimel, D.S., Kirchner, T., Menaut, J.C., Seastedt, T., Garcia Moya, E., Kamnalrut, A., and Kinyamario, J.I., 1993. Observations and modeling of biomass and soil organic matter dynamics for the grassland biome worldwide, *Global Biogeochemical Cycles*, 7, 785–809.
- Pendergrass, K.L., Miller, P.M., Kauffman, J.B., Kaye, T.N., 1999. The role of prescribed burning in maintenance of an endangered plant species, *Lomatium Bradshawii*. *Ecological Applications*, 9, 1420–1429.
- Peng, C., Liu, J., Dang, Q., Apps, M.J., and Jiang, H., 2002. TRIPLEX: A generic hybrid model for predicting forest growth and carbon and nitrogen dynamics, *Ecological Modelling*, 153, 109–130.
- Pistocchi A., Cassani, G. Zani, O., 2002. Use of the USPED model for mapping soil erosion and managing best land conservation practices, In Rizzoli, A. E. and Jakeman, A. J., (eds.), *Integrated Assessment and Decision Support, Proceedings of the First Biennial Meeting of the International Environmental Modelling and Software Society*, Vol. 1, pp. 163–168. iEMSs, 2002. <http://www.iemss.org/iemss2002/proceedings/>
- Potter, C.S. et al., 1993. Terrestrial ecosystem production: a process model based on global satellite and surface data, *Global Biogeochemical Cycles*, 7, 811–841.
- Prentice, I. C., 2001. The carbon cycle and atmospheric carbon dioxide, in *Climate Change 2001: The Scientific Basis*, edited by J. T. Houghton and Y. H. Ding, pp. 183–237, Cambridge Univ. Press, Cambridge.
- Ramankutty, N., Gibbs, H.K., Achard, F., Defriess, R., Foley, J.A., Houghton, R.A., 2007. Challenges to estimating carbon emissions from tropical deforestation, *Global Change Biology*, 13, 51–66.
- Reich, P.B., Peterson, D.W., Wedin, D.A., Wrage, K., 2001. Fire and vegetation effects on productivity and nitrogen cycling across a forest-grassland continuum. *Ecology*, 82, 1703–1719.

- Reiners, W. A., Liu, S., Gerow, K. G., Keller, M., and Schimel, D. S., 2002. Historical and future land use effects on trace gas emissions using an ensemble modeling approach: Costa Rica's Caribbean Lowlands as an example, *Global Biogeochemical Cycles*, 16, 1068, doi: 10.1029/2001GB001437.
- Renard, K.G., Forster, G.R., Weesies, G.A., McCool, D.K., Yoder, D.C. 1997. Predicting soil erosion by water: A guide to conservation planning with the Revised Universal Soil Loss Equation (RUSLE). USDA Agric. Handbook 703. U.S. Gov. Print. Office, Washington, D.C.
- Renard, K.G., Forster, G.R., Weesies, G.A., McCool, D.K., Yoder, D.C., 1997. Predicting soil erosion by water: A guide to conservation planning with the Revised Universal Soil Loss Equation (RUSLE). USDA Agric. Handbook 703. U.S. Gov. Print. Office, Washington, D.C.
- SAS. 2004. SAS Version 9.1. SAS Institute, Cary, North Carolina, USA.
- Schimel, D.S., Kittel, T.G.F., Parton, W.J., 1991. Terrestrial biogeochemical cycles: global interactions with the atmosphere and hydrology, *Tellus V*, 43AB, 188–203.
- Schimel, D., Kicklighter, D., Kittel, T., Rosenbloom, N., Running, S., Thornton, P., Ojima, D., Parton, W., Kelly, R., Sykes, H., Neilson, R., Rizzo, B., Helillo, J., Tian, H., and McGuire, A. D., 2000. Contribution of increasing CO₂ and climate to carbon storage by ecosystems in the United States, *Science*, 287, 2004–2006.
- Schimel, D.S., House, J.I., Hibbard, K.A. et al., 2001. Recent patterns and mechanisms of carbon exchange by terrestrial ecosystems, *Nature*, 414, 169–172.
- SCS. Technical Release 55: Urban Hydrology for Small Watersheds. USDA (U.S. Department of Agriculture). June 1986.
- SERDP SEMP annual report, 2003. http://www.cecer.army.mil/techreports/SEMP_FY03/SEMP_FY_2003_Technical_Report.pdf
- Sohl, T.L., Sayler, K.L., 2008. Using the FORE-SCE model to project land cover change in the southeastern United States, *Ecological Modelling*, 219, 49–65.
- Sohl, T.L., Sayler, K.L., Drummond, M.A., Loveland, T.R., 2007. The FORE-SCE model: A practical approach for projecting land use change using scenario-based modeling, *Journal of Land Use Science*, 1, 1–24.
- Tan Z., Liu, S.G., Johnston, C.A., Liu, J., Tieszen, L.L., 2006. Analysis of ecosystem controls on soil carbon source-sink relationships in the northwest Great Plains, *Global Biogeochemical Cycles*, 20, GB4012, doi:10.1029/2005GB002610.

- Tan Z., Liu, S.G., Li, Z., Loveland, T.R., 2007. Simulated responses of soil organic carbon stock to tillage management scenarios in the Northwest Great Plains, *Carbon Balance and Management*, 2, 7, doi:10.1186/1750-0680-2-7.
- Tan, Z., Liu, S.G., Johnston, C.A. et al., 2005. Soil organic carbon dynamics as related to land use history in the Northwestern Great Plains, *Global Biogeochemical Cycles*, 19, GB3011, doi:10.1029/2005GB002536.
- Towne, E.G., Knapp, A.K., 1996. Biomass and density responses in tallgrass prairie legumes to annual fire and topographic position. *American Journal of Botany*, 83, 175–179.
- VEMAP Members, 1995. Vegetation/ecosystem modeling and analysis project: comparing biogeography and biogeochemistry models in a continental-scale study of terrestrial ecosystem responses to climate change and CO₂ doubling, *Global Biogeochemical Cycles*, 9, 407–437.
- Wagle, R.F., Eakle, T.W., 1979. A controlled burn reduces the impact of a subsequent wild fire in ponderosa pine vegetation type. *Forest Science*, 25, 123–129.
- Waldrop, T.A., White, D.L., Jones, S.M., 1992. Fire regimes for pine grassland communities in the southeastern united-states. *Forest Ecology and Management*, 47, 195–210.
- Warren, S.D., Mitasova, H., Hohmann, M.G., Landsberger, S., Iskander, F. Y., Ruzycki, T. S. Senseman, G.M., 2005. Validation of a 3-D enhancement of the Universal Soil Loss Equation for prediction of soil erosion and sediment deposition. *Catena*, 64, 281–296.
- Zaluski, M.H., Consort, J.J., and Antonioli, S.B. 2003. Soil Erosion and Deposition Modeling in ArcGIS. In *Business and Industry Symposium*, 108–113. The Society for Modeling and Simulation International (SCS).

Appendices

A.1 Supporting Data

None

A.2 List of Technical Publications

Liu, J., Liu, S., Tieszen, L., Chen, M., 2007. Estimating Soil Erosion Using the USPED Model and Consecutive Remotely Sensed Land Cover Observations. Summer Computer Simulation Conference 2007 (SCSC 2007) , San Diego, California (USA), July 15–18, 2007.

Zhao, S., Liu, S., Tieszen, L., Imm, D., Burton, M., Balbach, H., 2007. Fort Benning Forest Status and Trends. SERDP and ESTCP's Partners in Environmental Technology, Technical Symposium & Workshop. Washington, D.C., December 4–6, 2007.

Liu, S., Zhao, S., Tieszen, L., Imm, D., Balbach, H., 2007. Simulated Impacts of Cyclic Fire On Ecosystem Carbon and Nitrogen Cycles at Fort Benning. SERDP and ESTCP's Partners in Environmental Technology, Technical Symposium & Workshop. Washington, D.C., December 4–6, 2007.

Liu, S., Liu, J., Zhao, S., Tieszen, L., 2007. Estimating Soil Erosion at Fort Benning Using the USPED Model and Consecutive Remotely Sensed Land Cover Observations. SERDP and ESTCP's Partners in Environmental Technology, Technical Symposium & Workshop. Washington, D.C., December 4–6, 2007.

Zhao, S., Liu, S., Li, Z., Sohl, T. Ignoring detailed fast-changing dynamics of land use overestimates regional terrestrial carbon sequestration, *Biogeosciences Discussions*, Volume 6, 2009, pp.3215–3235.

Zhao, S., Liu, S., Li, Z., Sohl, T. A spatial resolution threshold of land cover in estimating regional terrestrial carbon sequestration, *Biogeosciences Discussions*, Volume 6, 2009, pp.7983–8006.

Zhao, S., Liu, S., Li, Z., Sohl, T. Differences in carbon sequestration between a military installation (Fort Benning) and surrounding areas: a case study from the U.S. Southeast, *Journal of Geophysical Research -Biogeosciences*, (submitted).

A.3 Other Technical Material

GMES model flow chart and model setup

Original GEMS user guide (named “Emla”) and updates

Pre-processing (AML GUI code) and post-processing (summarization) codes.

CENTURY 4.0 manual, by which EDCM was adopted and modified, includes mathematical construct.